Inorganic Chemistry

ARTICLE

pubs.acs.org/IC

Heterobridged Dinuclear, Tetranuclear, Dinuclear-Based 1-D, and Heptanuclear-Based 1-D Complexes of Copper(II) Derived from a Dinucleating Ligand: Syntheses, Structures, Magnetochemistry, Spectroscopy, and Catecholase Activity

Samit Majumder,[†] Sohini Sarkar,[†] Sujit Sasmal,[†] E. Carolina Sañudo,*[,‡] and Sasankasekhar Mohanta*[,†]

[†]Department of Chemistry, University of Calcutta, 92 A. P. C. Road, Kolkata 700 009, India

[‡]Department de Química Inorgànica i Institut de Nanociència i Nanotecnologia, Universitat de Barcelona, Diagonal 647, 08028 Barcelona, Spain

Supporting Information

ABSTRACT: The work in this paper presents syntheses, characterization, crystal structures, variable-temperature/field magnetic properties, catecholase activity, and electrospray ionization mass spectroscopic (ESI-MS positive) study of five copper(II) complexes of composition $[Cu^{II}_2L(\mu_{1,1}\text{-}NO_3)(H_2O)(NO_3)](NO_3)$ (**1**), $[\{Cu^{II}_2L(\mu\text{-}OH)(H_2O)\}(\mu\text{-}ClO_4)]_n(ClO_4)_n$ (**2**), $[\{Cu^{II}_2L(NCS)_2\}(\mu_{1,3}\text{-}NCS)]_n$ (**3**), $[\{Cu^{II}_2L(\mu_{1,1}\text{-}N_3)(ClO_4)\}_2(\mu_{1,3}\text{-}N_3)_2]$ (**4**), and $[\{Cu^{II}_2L(\mu\text{-}OH)\}\{Cu^{II}_2L(\mu_{1,1}\text{-}N_3)\}\{Cu^{II}(\mu_{1,1}\text{-}N_3)_4(dmf)\}\{Cu^{II}_2(\mu_{1,1}\text{-}N_3)_2(N_3)_4\}]_n \cdot n$dmf (**5**), derived from a new compartmental ligand 2,6-bis[N-(2-pyridylethyl)formidoyl]-4-ethylphenol, which is the 1:2 condensation product of 4-ethyl-2,6-diformylphenol and 2-(2-aminoethyl)pyridine. The title compounds are either of the following nuclearities/topologies: dinuclear (**1**), dinuclear-based one-dimensional (**2** and **3**), tetranuclear (**4**), and heptanuclear-based one-dimensional (**5**). The bridging moieties in **1**−**5** are as follows: μ-phenoxo-$\mu_{1,1}$-nitrate (**1**), μ-phenoxo-μ-hydroxo and μ-perchlorate (**2**), μ-phenoxo and $\mu_{1,3}$-thiocyanate (**3**), μ-phenoxo-$\mu_{1,1}$-azide and $\mu_{1,3}$-azide (**4**), μ-phenoxo-μ-hydroxo, μ-phenoxo-$\mu_{1,1}$-azide, and $\mu_{1,1}$-azide (**5**). All the five compounds exhibit overall antiferromagnetic interaction. The J values in **1**−**4** have been determined (-135 cm^{-1} for **1**, -298 cm^{-1} for **2**, -105 cm^{-1} for **3**, -119.5 cm^{-1} for **4**). The pairwise interactions in **5** have been evaluated qualitatively to result in $S_T = 3/2$ spin ground state, which has been verified by magnetization experiment. Utilizing 3,5-di-*tert*-butyl catechol (3,5-DTBCH$_2$) as the substrate, catecholase activity of all the five complexes have been checked. While **1** and **3** are inactive, complexes **2**, **4**, and **5** show catecholase activity with turn over numbers 39 h^{-1} (for **2**), 40 h^{-1} (for **4**), and 48 h^{-1} (for **5**) in dmf and 167 h^{-1} (for **2**) and 215 h^{-1} (for **4**) in acetonitrile. Conductance of the dmf solution of the complexes has been measured, revealing that bridging moieties and nuclearity have been almost retained in solution. Electrospray ionization mass (ESI-MS positive) spectra of complexes **1**, **2**, and **4** have been recorded in acetonitrile solutions and the positive ions have been well characterized. ESI-MS positive spectrum of complex **2** in presence of 3,5-DTBCH$_2$ have also been recorded and, interestingly, a positive ion $[Cu^{II}_2L(\mu\text{-}3,5\text{-}DTBC^{2-})(3,5\text{-}DTBCH^{-})Na^{I}]^+$ has been identified.

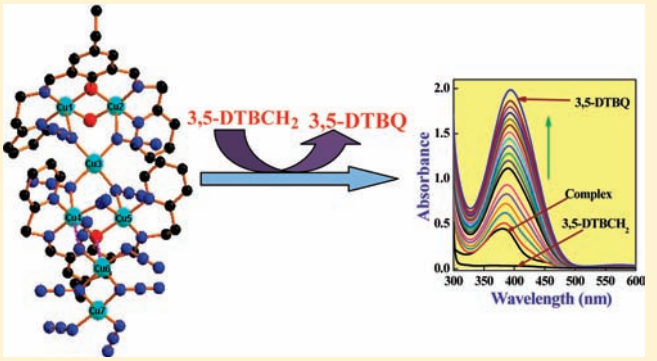

INTRODUCTION

Some of the important aspects in coordination chemistry research are rational design of organic blocking ligands and utilization of organic/inorganic bridging ligands to develop metal−organic molecules, including dinuclear systems, oligo- and polynuclear clusters, and 1-D, 2-D, and 3-D self-assemblies, having interesting properties relevant to the frontier areas such as molecular magnetism,[1−10] supramolecular chemistry/crystal engineering,[3a,11,12] and modeling the active sites of metallo-enzymes.[13−21]

To develop varieties of topologies, pseudohalides like azide[1a,3a−3d] and thiocyanate[3e] are known to behave excellently as bridging ligands. Metallo-azide species, in particular, have been always of great interest in supramolecular chemistry/crystal engineering and molecular magnetism because of a number of coordination modes of this potentially bridging ligand as well as because of its ability to mediate ferro- or antiferromagnetic interactions among metal centers. However, in spite of the considerable amount of information available, it is quite difficult to control/predict composition and topology of a new metallo-azide compound because, for a particular metal ion, the final product is primarily dependent on the organic ligand(s) and also on the reaction conditions. Clearly, new types of composition and topology may be achieved on utilizing new organic ligands.

Received: February 28, 2011
Published: July 21, 2011

Catechol oxidase is an enzyme with the type-3 active site that catalyzes the oxidation of a wide range of *o*-diphenols (catechols) to the corresponding *o*-quinones coupled with $2e/2H^+$ reduction of O_2 to H_2O, in a process known as catecholase activity.[13−22] The crystal structure of the met form of the enzyme was determined in 1998 revealing that the active center consists of a hydroxo-bridged dicopper(II) center in which each copper(II) center is coordinated to three histidine nitrogens and adopts a trigonal pyramidal environment with one nitrogen in the apical site.[13f] The structure determination of catecholase oxidase has encouraged an extensive investigation on model compounds to understand the structure−property relationship.[5b,13a−13c,14b−14f,15−21] As the structure contains dicopper(II) moiety, several dicopper(II) complexes derived from nitrogen-containing dinucleating ligands have been mainly employed for this purpose. Several monocopper(II) complexes are also known to exhibit the activity. Recently, catecholase activity of complexes of other metal ions, Mn for example, has also been observed.[18] Moreover, few structure−property correlations that were determined are not sufficiently wide but only applicable for a set of few compounds.[5b,9d,13,14,19,20] All in all, the problem of modeling the catecholase activity remains open, and therefore, catecholase activity of new systems should be explored to get better insight and more straightforward structure−property correlations.

On transforming both the dialdehyde moieties of 4-substituted-2,6-diformylphenol to imine or amine functionality, a number of dinucleating acyclic ligands having monophenoxo bridging ability have been reported previously.[5b,9d,13a−13c,14a−14d,21−25] In terms of the set of donor atoms to accommodate two metal ions, the combination of the two sites of these ligands is usually NO−NO, N_2O-N_2O, N_3O-N_3O, or $N_2O_2-N_2O_2$. As the donor centers of both of the two sites cannot satisfy the required coordination number of the metal ions, these ligands are excellent systems to stabilize heterobridged metal complexes having bridging moieties like μ-phenoxo-μ-X, μ-phenoxo-bis(μ-X), μ-phenoxo-μ-X-μ-Y, etc. (X/Y = chloro, bromo, hydroxo, methoxy, azide, cyanate, perchlorate, carboxylate, pyrazolate, etc.).[5b,9d,13a−13c,14a−14d,21−25] Regarding copper(II) complexes derived from such ligands, several double- or triple-bridged dicopper(II) compounds have been reported.[5b,9d,13a−13c,14a−14d,21−25] Utilizing dicarboxylates and dipyridines having 4,4′-bipyridine functionality as the second bridging ligand, a few tetracopper(II) systems are also known.[24] A few polymeric copper(II) compounds have also been reported where the heterobridged dicopper(II) cores are interlinked by bridging ligands (azide, alkoxo, etc.).[25] Catecholase oxidase activity of some of these dicopper(II) systems have been investigated,[5b,9d,13a−13c,14a−14d,21,22] while magnetic studies have been carried out for some of these di-, tetra- and polynuclear systems.[5b,9d,21,23−25] To explore the copper(II) compounds derived from similar but new dinucleating acyclic ligands, we have synthesized 2,6-bis[N-(2-pyridylethyl)formidoyl]-4-ethylphenol (HL; Chart 1) and utilized it to prepare five copper(II) compounds $[Cu^{II}_2L(\mu_{1,1}\text{-}NO_3)(H_2O)(NO_3)](NO_3)$ (**1**), $[\{Cu^{II}_2L(\mu\text{-}OH)(H_2O)\}(\mu\text{-}ClO_4)]_n(ClO_4)_n$ (**2**), $[\{Cu^{II}_2L(NCS)_2\}(\mu_{1,3}\text{-}NCS)]_n$ (**3**), $[\{Cu^{II}_2L(\mu_{1,1}\text{-}N_3)(ClO_4)\}_2(\mu_{1,3}\text{-}N_3)_2]$ (**4**), and $[\{Cu^{II}_2L(\mu\text{-}OH)\}\{Cu^{II}_2L(\mu_{1,1}\text{-}N_3)\}\{Cu^{II}(\mu_{1,1}\text{-}N_3)_4(dmf)\}\{Cu^{II}_2(\mu_{1,1}\text{-}N_3)_2(N_3)_4\}]_n\cdot n$dmf (**5**). Herein, we report syntheses, characterization by FT-IR and molar conductance data, crystal structures, magnetic properties, catecholase activity, and electrospray ionization mass spectroscopic (ESI-MS positive) studies of these five compounds.

Chart 1. Chemical Structure of HL

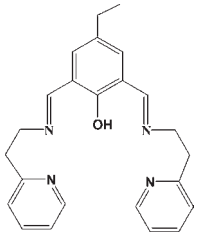

EXPERIMENTAL SECTION

Materials and Physical Measurements. All the reagents and solvents were purchased from commercial sources and used as received. 2,6-Diformyl-4-ethylphenol was prepared according to the procedure reported for the synthesis of 2,6-diformyl-4-methylphenol.[26] Elemental (C, H, and N) analyses were performed on a Perkin-Elmer 2400 II analyzer. IR spectra were recorded in the region 400−4000 cm^{-1} on a Bruker-Optics Alpha-T spectrophotometer with samples as KBr disks. Magnetic susceptibility measurements were carried out on polycrystalline samples with a DSM5 Quantum Design magnetometer working in the range of 2−300 K under magnetic field of 1 T. Diamagnetic corrections were estimated from Pascal Table. Electronic spectroscopic measurements and catecholase activity were performed with a Hitachi U-3501 spectrophotometer. The electrospray ionization mass (ESI-MS positive) spectra were recorded on a Micromass Qtof YA 263 mass spectrometer. Molar conductivity (Λ_M) of 1 mM solution in dmf was measured at 25 °C with a Systronics conductivity bridge.

Syntheses 2,6-Bis[N-(2-pyridylethyl)formidoyl]-4-ethylphenol (HL) Solution in Methanol. 2,6-Diformyl-4-ethylphenol (1.780 g, 10 mmol) and 2-(2-aminoethyl)pyridine (2.443 g, 20 mmol) were dissolved in 50 mL methanol, and the mixture was refluxed for 2 h. After cooling and filtration to remove the suspended particles, the volume of the solution was adjusted to 100 mL. This "solution of HL" was considered to contain 10 mmol of the ligand HL and was used for subsequent reactions without further purification.

$[Cu^{II}_2L(\mu_{1,1}\text{-}NO_3)(H_2O)(NO_3)](NO_3)$ (1). Ten milliliters of the "solution of HL" containing 1 mmol HL was taken and diluted to 30 mL with methanol. To this solution were dropwise added successively a methanol (10 mL) solution of triethylamine (0.101 g, 1 mmol) and an acetonitrile solution (15 mL) of copper(II) nitrate trihydrate (0.482 g, 2 mmol), and the resulting deep green solution was refluxed for 2 h. Then the mixture was filtered, and the filtrate was kept at room temperature for slow evaporation. After 2−3 days, a deep green crystalline compound containing diffraction quality single crystals was deposited, which was collected by filtration, washed with cold methanol, and air-dried. Yield: 0.57 g (80%). Anal. Calcd for (%) $C_{24}H_{27}N_7O_{11}Cu_2$: C, 40.23; H, 3.80; N, 13.68. Found: C, 40.19; H, 3.82; N, 13.72. IR (KBr pellet, cm^{-1}): $\nu(H_2O)$, 3417(b); $\nu(C{=}N)$, 1645(s); $\nu(NO_3)$, 1385 (vs), 1279(s). UV−vis (DMF) λmax/nm (ε in M^{-1} cm^{-1}): 267 (34287), 374 (8680), 648 (145).

$[\{Cu^{II}_2L(\mu\text{-}OH)(H_2O)\}(\mu\text{-}ClO_4)]_n(ClO_4)_n$ (2). To a 10 mL "solution of HL" containing 1 mmol HL were dropwise added successively under stirring a methanol (10 mL) solution of triethylamine (0.101 g, 1 mmol) and a methanol (10 mL) solution of copper(II) perchlorate hexahydrate (0.744 g, 2 mmol). Immediately, a green compound started to deposit. After stirring for 2 h, the green solid was collected by filtration and washed with methanol. Recrystallization from an acetonitrile−toluene (1:2) mixture produced a green crystalline compound containing diffraction quality single crystals. Yield: 0.56 g (75%). Anal. Calcd for (%) $C_{24}H_{28}N_4O_{11}Cl_2Cu_2$: C, 38.62; H, 3.78; N, 7.51. Found: C, 38.57; H, 3.75; N, 7.50. IR (KBr pellet, cm^{-1}): $\nu(H_2O)$, 3510(b); $\nu(C{=}N)$,

dx.doi.org/10.1021/ic200409d |*Inorg. Chem.* 2011, 50, 7540–7554

Table 1. Crystallographic Data for 1−5

	1	2	3	4	5
empirical formula	$C_{24}H_{27}N_7O_{11}Cu_2$	$C_{24}H_{22}N_4O_{11}Cl_2Cu_2$	$C_{27}H_{25}N_7OS_3Cu_2$	$C_{48}H_{50}N_{20}O_{10}Cl_2Cu_4$	$C_{54}H_{64}N_{43}O_5Cu_7$
formula weight	716.61	740.44	686.80	1392.14	1840.26
crystal system	triclinic	orthorhombic	monoclinic	triclinic	triclinic
space group	$P\bar{1}$	*Pbca*	*Cc*	$P\bar{1}$	*P*1
a (Å)	10.169(5)	17.3516(7)	12.4131(4)	8.9895(2)	11.5844(10)
b (Å)	11.127(5)	14.5574(6)	26.1746(8)	12.0401(3)	11.9880(10)
c (Å)	13.182(6)	22.5361(9)	8.7937(3)	13.2996(3)	14.8922(13)
α (°)	94.846(12)	90.00	90.00	73.8450(10)	106.7910(10)
β (°)	104.436(11)	90.00	91.7770(10)	86.4900(10)	104.2630(10)
γ (°)	105.468(11)	90.00	90.00	74.2360(10)	107.7670(10)
V (Å^3)	1373.8(11)	5692.5(4)	2855.77(16)	1330.47(5)	1754.0(3)
Z	2	8	4	1	1
D (calculated, g cm^{-3})	1.732	1.728	1.597	1.738	1.742
λ (Mo K$_α$), Å	0.71073	0.71073	0.71073	0.71073	0.71073
μ (mm^{-1})	1.623	1.748	1.744	1.757	2.162
T (K)	293(2)	100(2)	293(2)	293(2)	100(2)
F(000)	732	2992	1400	708	932
2*θ* range for data collection (°)	3.24−52.58	3.62−50.76	3.12−61.08	3.18−56.60	3.08−50.66
index ranges	$-12 \le h \le 12$	$-20 \le h \le 20$	$-17 \le h \le 17$	$-11 \le h \le 11$	$-13 \le h \le 13$
	$-13 \le k \le 13$	$-17 \le k \le 17$	$-33 \le k \le 35$	$-16 \le k \le 16$	$-14 \le k \le 14$
	$-16 \le l \le 16$	$-27 \le l \le 27$	$-12 \le l \le 11$	$-17 \le l \le 17$	$-17 \le l \le 17$
no. measured reflections	17262	64647	21254	19187	12925
no. independent reflections	5485	5226	7262	6316	9863
R_{int}	0.0583	0.0748	0.0338	0.0264	0.0425
no. refined parameters	505	428	449	479	936
no. observed reflections, $I \ge 2\sigma(I)$	4031	4007	6170	5365	7655
goodness-of-fit on F^2, *S*	0.907	1.113	1.002	1.088	1.038
R_1[a], wR_2[b] [$I \ge 2\sigma(I)$]	0.0438, 0.1235	0.0635, 0.1274	0.0307, 0.0494	0.0304, 0.0581	0.0627, 0.1361
R_1[a], wR_2[b] [all data]	0.0677, 0.1399	0.0856, 0.1380	0.0435, 0.0526	0.0386, 0.0605	0.0870, 0.1514
max, min electron density (eÅ^{-3})	0.675, −0.654	0.843, −1.114	0.412, −0.451	0.558, −0.489	1.514, −1.388

[a] $R_1 = [\Sigma||F_o| - |F_c||/\Sigma|F_o|]$. [b] $wR_2 = [\Sigma w(F_o^2 - F_c^2)^2/\Sigma wF_o^4]^{1/2}$.

1642(s); $\nu(ClO_4)$, 1111(vs), 624(w). UV−vis (DMF) λmax/nm (ε in M^{-1} cm^{-1}): 267 (33980), 384 (7360), 635 (130).

[{Cu$^{II}_2$L(NCS)$_2$}(μ$_{1,3}$-NCS)]$_n$ (3). To a stirred 10 mL "solution of HL" containing 1 mmol HL were dropwise added successively a methanol (10 mL) solution of triethylamine (0.101 g, 1 mmol) and a methanol (10 mL) solution of copper(II) perchlorate hexahydrate (0.744 g, 2 mmol). The resulting green solution was refluxed for 0.5 h, and then to the refluxed solution was added an aqueous (5 mL) solution of ammonium thiocyanate (0.304 g, 4 mmol). Immediately, a brown solid started to deposit. After refluxing for additional 2 h, the deposited solid was collected by filtration and washed with methanol. Recrystallization on diffusion diethyl ether into a *N*,*N*-dimethylformamide (dmf) solution in long tubes produced a brown crystalline compound containing diffraction quality single crystals. Yield: 0.48 g (70%). Anal. Calcd for (%) $C_{27}H_{25}N_7OS_3Cu_2$: C, 47.22; H, 3.67; N, 14.27. Found: C, 47.25; H, 3.64; N, 14.28. IR (KBr pellet, cm^{-1}): ν(SCN), 2082(vs); ν(C═N), 1638(s). UV−vis (DMF) λmax/nm (ε in M^{-1} cm^{-1}): 266 (34305), 368 (6280), 660 (154).

[{Cu$^{II}_2$L(μ$_{1,1}$-N$_3$)(ClO$_4$)}$_2$(μ$_{1,3}$-N$_3$)$_2$] (4), and [{Cu$^{II}_2$L(μ-OH)}{Cu$^{II}_2$L(μ$_{1,1}$-N$_3$)}{Cu^{II}(μ$_{1,1}$-N$_3$)$_4$(dmf)}{Cu$^{II}_2$(μ$_{1,1}$-N$_3$)$_2$-(N$_3$)$_4$}]$_n$·*n*dmf (5). To a mixture of a 10 mL "solution of HL" containing 1 mmol HL, a methanol (10 mL) solution of triethylamine (0.101 g, 1 mmol), and a methanol (10 mL) solution of copper(II) perchlorate hexahydrate (0.744 g, 2 mmol), an aqueous solution (5 mL) of sodium azide (0.260 g, 4 mmol) was added under reflux. Immediately, a brown compound started to deposit. Reflux was continued for 2 h, and then the mixture was filtered to give rise a brown solid and a deep green filtrate. The brown solid was recrystallized on diffusing diethyl ether into a dmf solution in long tubes to produce brown crystalline compound **5** containing diffraction quality single crystals. On the other hand, the deep green filtrate was evaporated on a rotary evaporator to give rise a deep green solid, which was collected after washing with methanol−water (1:2) mixture. This deep green mass was recrystallized from an acetonitrile−toluene (1:2) mixture to produce a deep green crystalline compound **4** containing diffraction quality crystals. Data of **4**: Yield: 0.35 g (25%). Anal. Calcd for (%) $C_{48}H_{50}N_{20}O_{10}Cl_2Cu_4$: C, 41.41; H, 3.62; N, 20.12. Found: C, 41.39; H, 3.59; N, 20.15. IR (KBr pellet, cm^{-1}): $\nu(N_3)$, 2082(s), 2041(s); ν(C═N), 1644(s); $\nu(ClO_4)$, 1091(s), 622(w). UV−vis (DMF) λmax/nm (ε in M^{-1} cm^{-1}): 267 (33567), 384 (15600), 713 (390). Data of **5**: Yield: 0.65 g (35%). Anal. Calcd for (%) $C_{54}H_{65}N_{43}O_5Cu_7$: C, 35.23; H, 3.56; N, 32.71. Found: C, 35.25; H, 3.64; N, 32.65. IR (KBr pellet, cm^{-1}): $\nu(N_3)$, 2069(s), 2034(s); ν(C═N), 1643(s). UV−vis (DMF) λmax/nm (ε in M^{-1} cm^{-1}): 267 (33960), 380 (17800), 707 (634).

Crystal Structure Determination of 1−5. The crystallographic data for **1**−**5** are summarized in Table 1. Diffraction data were collected on a Bruker-APEX II SMART CCD diffractometer at 293 K for **1**, **3**, and **4** and at 100 K for **2** and **5** using graphite-monochromated Mo Kα radiation (λ = 0.71073 Å). For data processing and absorption correction the packages SAINT[27a] and SADABS[27b] were used. The structures

dx.doi.org/10.1021/ic200409d |*Inorg. Chem.* 2011, 50, 7540–7554

were solved by direct and Fourier methods and refined by full-matrix least-squares based on F^2 using SHELXTL[27c] and SHELXL-97[27d] packages.

During the development of the structures of **2** and **5**, it became apparent that few atoms were each disordered over two sites. These disordered atoms are C18, N4, O6, O7, O10, and O11 for **2** and N34 and N35 for **5**. This was allowed for refining freely, and the final linked occupancy parameters for these disordered atoms are 0.74 and 0.26 for C18; 0.63 and 0.37 for N4; 0.71 and 0.29 for O6; 0.61 and 0.39 for O7; 0.86, and 0.14 for O10; 0.93 and 0.07 for O11; and 0.60 and 0.40 for N34 and N35.

All the hydrogen atoms in **1** and **4** were located, while all the hydrogen atoms in **5** were inserted at calculated positions with isotropic thermal parameters. In **2**, it was not possible to either locate or insert six hydrogen atoms: two linked with the water oxygen atom, one linked with the hydroxo oxygen atom, two linked with C18, and one of two linked with C19. All other hydrogen atoms in **2** were inserted at calculated positions with isotropic thermal parameters. In **3**, two hydrogen atoms (H7A and H7B) linked with C7 and one hydrogen atom (H22) linked with C22 were inserted at calculated positions with isotropic thermal parameters. All other hydrogen atoms in **3** were located.

Because of the nonpositive definite problem, few nonhydrogen atoms in the structures of **2** and **5** had to be refined isotropically. These atoms are O10A, O11A, and C18A for **2** and C15, C26, C34, C35, C38, C41, C44, N9, N21, N25, N27, N40, N34A, and N35A for **5**. All other nonhydrogen atoms in **2** and **5** and all the nonhydrogen atoms in **1**, **3**, and **4** were refined anisotropically, while all the hydrogen atoms in **1**−**5** were refined isotropically. The final refinements converged at the R_1 values ($I > 2\sigma(I)$) 0.0438, 0.0635, 0.0307, 0.0304, and 0.0627 for **1**, **2**, **3**, **4**, and **5**, respectively.

RESULTS AND DISCUSSION

Syntheses, FT-IR Spectra, and Proposed Composition in Solution. In the reaction of HL with copper(II) nitrate and copper(II) perchlorate in the presence of the base, Et_3N, the exogeneous position is occupied by a nitrate and a hydroxo anions to result in the formation of compounds $[Cu^{II}_2L(\mu_{1,1}\text{-}NO_3)(H_2O)(NO_3)](NO_3)$ (**1**) and $[\{Cu^{II}_2L(\mu\text{-}OH)(H_2O)\}(\mu\text{-}ClO_4)]_n(ClO_4)_n$ (**2**), respectively. When HL in the presence of Et_3N is treated with copper(II) perchlorate and sodium azide, two compounds $[\{Cu^{II}_2L(\mu_{1,1}\text{-}N_3)(ClO_4)\}_2(\mu_{1,3}\text{-}N_3)_2]$ (**4**) and $[\{Cu^{II}_2L(\mu\text{-}OH)\}\{Cu^{II}_2L(\mu_{1,1}\text{-}N_3)\}\{Cu^{II}(\mu_{1,1}\text{-}N_3)_4(dmf)\}\{Cu^{II}_2(\mu_{1,1}\text{-}N_3)_2(N_3)_4\}]_n\cdot n$dmf (**5**) are produced. It may be noted that it was not possible to isolate HL in solid state; evaporation of solvent from even at high vacuum results in an orange oil, which contains mostly HL contaminated with some minor impurity(ies) as evidenced from its ^{1}H NMR spectrum.

The characteristic C═N stretching in compounds **1**−**5** appear as a strong band at about 1640 cm^{-1}. Presence of nitrates in compound **1** is evident by the observation of two strong bands at 1385 and 1279 cm^{-1}. The characteristic perchlorate vibrations are observed at 1111 and 624 cm^{-1} for **2** and at 1091 and 622 cm^{-1} for **4**. Two strong bands at 2082 and 2041 cm^{-1} for **4** and at 2069 and 2034 cm^{-1} for **5** are indicative of the presence of azide and more than one type of azide in both these molecules. The strong peak at 2082 cm^{-1} in the spectrum of **3** appears due to thiocyanate stretching. The presence of water molecules in compounds **1** and **2** is evident by the appearance of broad bands centered at 3417 cm^{-1} for **1** and at 3510 cm^{-1} for **2**.

To understand the composition in solution, molar conductance of the 10^{-3} (M) dmf solution of complexes **1**−**5** were measured. The conductance (Ω^{-1} cm^2 M^{-1}) values at 298 K for **1**−**5** are 185, 150, 92, 180, and 73, indicating that **1**, **2**, and **4** behave as 2:1 electrolytes, while **3** and **5** behave as 1:1 electrolytes in solution.[28] It is probable that in solution some of the long apical bonds (vide infra) are ruptured, and the vacant positions are occupied by solvent molecules (S). For example, the apical monodentate nitrate ion is probably eliminated from $[Cu^{II}_2L(\mu_{1,1}\text{-}NO_3)(H_2O)(NO_3)](NO_3)$ (**1**) to produce the 2:1 electrolyte $[Cu^{II}_2L(\mu_{1,1}\text{-}NO_3)(H_2O)(S)](NO_3)_2$. Similarly, the coordinated perchlorate ion is probably eliminated from $[\{Cu^{II}_2L(\mu\text{-}OH)(H_2O)\}(\mu\text{-}ClO_4)]_n(ClO_4)_n$ (**2**) to produce 2:1 electrolyte $[\{Cu^{II}_2L(\mu\text{-}OH)(H_2O)(S)_2](ClO_4)_2$. In the case of compound $[\{Cu^{II}_2L(\mu_{1,1}\text{-}N_3)(ClO_4)\}_2(\mu_{1,3}\text{-}N_3)_2]$ (**4**), which is neutral according to solid state composition, two axial perchlorate ions are most probably eliminated to produce the 2:1 electrolyte $[\{Cu^{II}_2L(\mu_{1,1}\text{-}N_3)(S)\}_2(\mu_{1,3}\text{-}N_3)_2](ClO_4)_2$, which is a better probable than another 2:1 electrolyte $[\{Cu^{II}_2L(\mu_{1,1}\text{-}N_3)(S)_n](ClO_4/N_3)_2$. The 1:1 electrolyte species in the case of $[\{Cu^{II}_2L(NCS)_2\}(\mu_{1,3}\text{-}NCS)]_n$ (**3**) is most probably $[\{Cu^{II}_2L(NCS)_2\}(S)_2](NCS)$, in which the bridging, which is also apical, thiocyanate moiety of the parent molecule is eliminated. As discussed below, $[\{Cu^{II}_2L(\mu\text{-}OH)\}\{Cu^{II}_2L(\mu_{1,1}\text{-}N_3)\}\{Cu^{II}(\mu_{1,1}\text{-}N_3)_4(dmf)\}\{Cu^{II}_2(\mu_{1,1}\text{-}N_3)_2(N_3)_4\}]_n\cdot n$dmf (**5**) can be considered as a self-assembly of a pentanuclear unit and a dinuclear unit, which are interlinked by semicoordination. It is logical that the semicoordination is ruptured in solution to produce a composition $[\{Cu^{II}_2L(\mu\text{-}OH)\}\{Cu^{II}_2L(\mu_{1,1}\text{-}N_3)(S)\}\{Cu^{II}(\mu_{1,1}\text{-}N_3)_4\}(S)_n]^{2+}$-$[\{Cu^{II}_2(\mu_{1,1}\text{-}N_3)_2(N_3)_4\}(S)_n]^{2-}$, which is a 1:1 electrolyte.

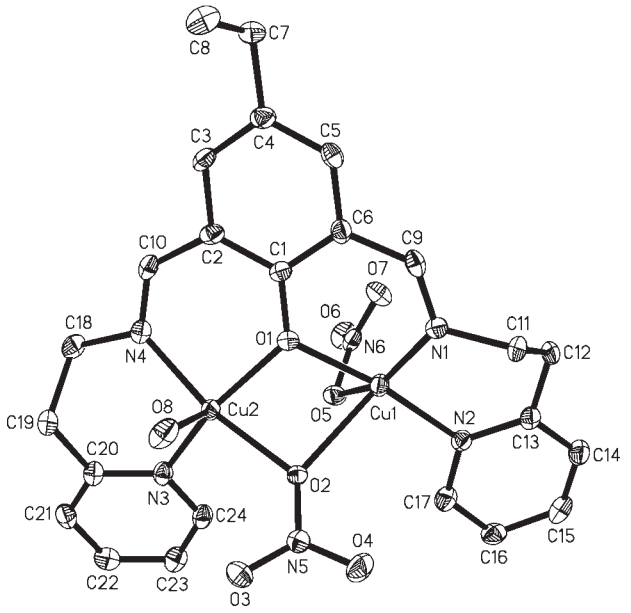

Figure 1. Crystal structure of complex $[Cu^{II}_2L(\mu_{1,1}\text{-}NO_3)(H_2O)(NO_3)](NO_3)$ (**1**). Counter nitrate anion and all the hydrogen atoms are omitted for clarity.

Description of Structures of $[Cu^{II}_2L(\mu_{1,1}\text{-}NO_3)(H_2O)(NO_3)](NO_3)$ (1), $[\{Cu^{II}_2L(\mu\text{-}OH)(H_2O)\}(\mu\text{-}ClO_4)]_n(ClO_4)_n$ (2), $[\{Cu^{II}_2L(NCS)_2\}(\mu_{1,3}\text{-}NCS)]_n$ (3), $[\{Cu^{II}_2L(\mu_{1,1}\text{-}N_3)(ClO_4)\}_2(\mu_{1,3}\text{-}N_3)_2]$ (4), and $[\{Cu^{II}_2L(\mu\text{-}OH)\}\{Cu^{II}_2L(\mu_{1,1}\text{-}N_3)\}\{Cu^{II}(\mu_{1,1}\text{-}N_3)_4(dmf)\}\{Cu^{II}_2(\mu_{1,1}\text{-}N_3)_2(N_3)_4\}]_n\cdot n$dmf (5). All these five complexes contain L^-, which has two N_2O compartments. Each of these compartments has one pyridine nitrogen and one imine nitrogen atoms and a common phenoxo oxygen atom. In all the five complexes, L^- acts as a dinucleating ligand by incorporating one copper(II) ion in each N_2O compartment. Clearly, phenoxo

dx.doi.org/10.1021/ic200409d |Inorg. Chem. 2011, 50, 7540–7554

oxygen atom in these complexes provides an endogeneous bridge for two copper(II) centers and L^- satisfies three coordination positions of each of the two metal ions.

The crystal structure of $[Cu^{II}_2L(\mu_{1,1}\text{-}NO_3)(H_2O)(NO_3)](NO_3)$ (**1**) is shown in Figure 1. The structure reveals that it is a heterobridged μ-phenoxo-$\mu_{1,1}$-nitrate dicopper(II) compound in which the metal centers are doubly bridged by the phenoxo oxygen atom of L^- and one oxygen atom of a bridging nitrate ion. Both the metal centers are pentacoordinated; the fifth coordination positions of Cu1 and Cu2 are occupied by one oxygen atom of a monodentate nitrate anion and a water molecule, respectively. Interestingly, compound **1** is the only example of a heterobridged μ-phenoxo-μ-nitrate dicopper(II) system.

The structure of $[\{Cu^{II}_2L(\mu\text{-}OH)(H_2O)\}(\mu\text{-}ClO_4)]_n(ClO_4)_n$ (**2**) is shown in Figure 2 and Figure S1 of the Supporting Information. The structure reveals that compound **2** is a dicopper(II)-based one-dimensional polymer. In the dinuclear core, the metal centers are doubly bridged by an endogeneous phenoxo atom of L^- and an exogeneous hydroxo oxygen atom. One metal center, Cu2, is pentacoordinated; a water oxygen atom (O3) occupies the fifth position. On the other hand, Cu1 is hexacoordinated due to the coordination of two perchlorate oxygen atoms, O5B and O7C, of two different perchlorate anions. Another oxygen atom (O7B and O5C) of each of these two perchlorate anions coordinates to two different copper(II) centers (Cu1H and Cu1D), which are symmetry related to Cu1, of two different dinuclear units to generate a dicopper(II)-based one-dimensional polymeric structure in **2** (Figure S1 of the Supporting Information).

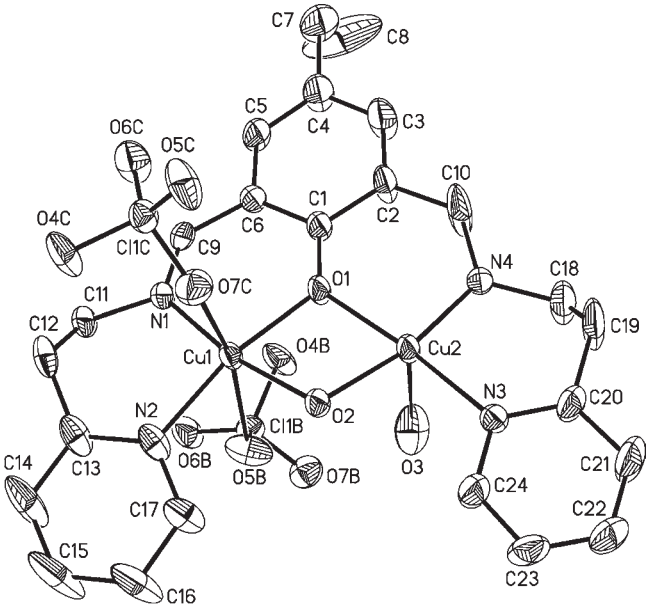

Figure 2. Crystal structure of complex $[\{Cu^{II}_2L(\mu\text{-}OH)(H_2O)\}(\mu\text{-}ClO_4)]_n(ClO_4)_n$ (**2**). All the hydrogen atoms are omitted for clarity. Symmetry code: B, $0.5 - x, y - 0.5, 1 + z$; C, $x, y - 1, 1 + z$.

As shown in Figure 3, $[\{Cu^{II}_2L(NCS)_2\}(\mu_{1,3}\text{-}NCS)]_n$ (**3**) is a monophenoxo-bridged dicopper(II)-based one-dimensional polymer. In the dinuclear unit, two metal centers are singly bridged by the phenoxo oxygen of L^-. Each of the two metal centers is coordinated to a terminal N-coordinated NCS^- anion. The fifth coordination position of Cu2 is occupied by the nitrogen atom of another NCS^- anion, the sulfur atom of which coordinates to a copper(II) center, Cu1B, of a neighboring dicopper(II) unit. Clearly, as shown in Figure 3, one monophenoxo-bridged dicopper(II) unit is interlinked with two neighboring symmetry related dinuclear units due to the bridging NCS^- ligand to result in the generation of a one-dimensional polymeric structure in compound **3**. It is evident also that both the metal centers are pentacoordinated with a N_3OS and a N_4O coordination environments for Cu1 and Cu2, respectively.

As shown in Figure 4, $[\{Cu^{II}_2L(\mu_{1,1}\text{-}N_3)(ClO_4)\}_2(\mu_{1,3}\text{-}N_3)_2]$ (**4**) is a tetracopper(II) compound. This tetracopper(II) system may be considered to consist of two symmetry related dicopper(II) units, of composition $[Cu^{II}_2L(\mu_{1,1}\text{-}N_3)(ClO_4)]^+$, interlinked by two end-to-end bridging azide anions. In the dicopper(II) unit, the two metal centers are doubly bridged by a phenoxo oxygen atom of L^- and a nitrogen atom of an end-on azide anion. One end-to-end azide anion bridges two metal centers, Cu1 and Cu2A, of two dinuclear units. Obviously, a symmetry related end-to-end azide anion bridges the second metal centers, Cu2 and Cu1A, of the same two dinuclear units. Clearly, two heterobridged μ-phenoxo-$\mu_{1,1}$-N_3 dicopper(II) units are interlinked by two end-to-end

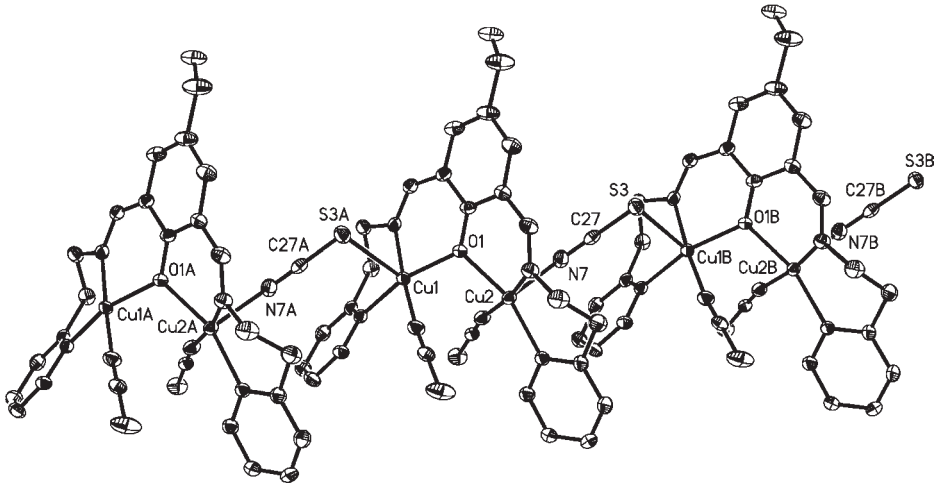

Figure 3. Perspective view of complex $[\{Cu^{II}_2L(NCS)_2\}(\mu_{1,3}\text{-}NCS)]_n$ **3** showing the dicopper(II)-based one-dimensional structure. Symmetry code: A, $x, y, 1 + z$; B, $x, y, z - 1$.

dx.doi.org/10.1021/ic200409d |*Inorg. Chem.* 2011, 50, 7540–7554

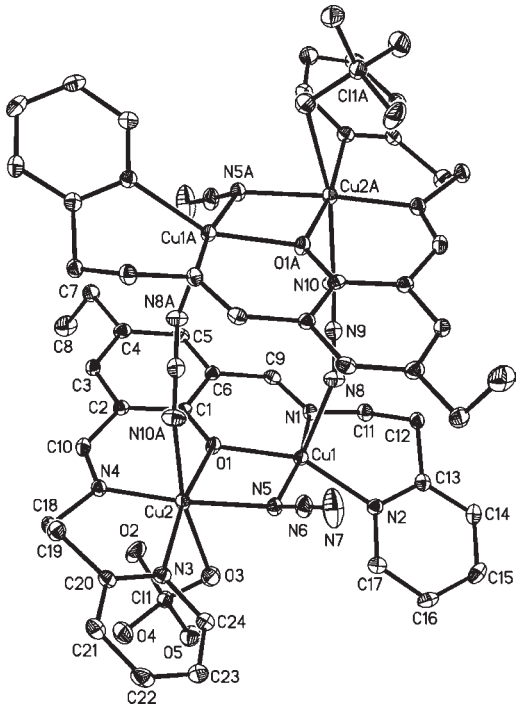

Figure 4. Crystal structure of complex $[\{Cu^{II}_2L(\mu_{1,1}\text{-}N_3)(ClO_4)\}_2(\mu_{1,3}\text{-}N_3)_2]$ (**4**). All the hydrogen atoms are omitted for clarity. Symmetry code: A, $1 - x$, $1 - y$, $-z$.

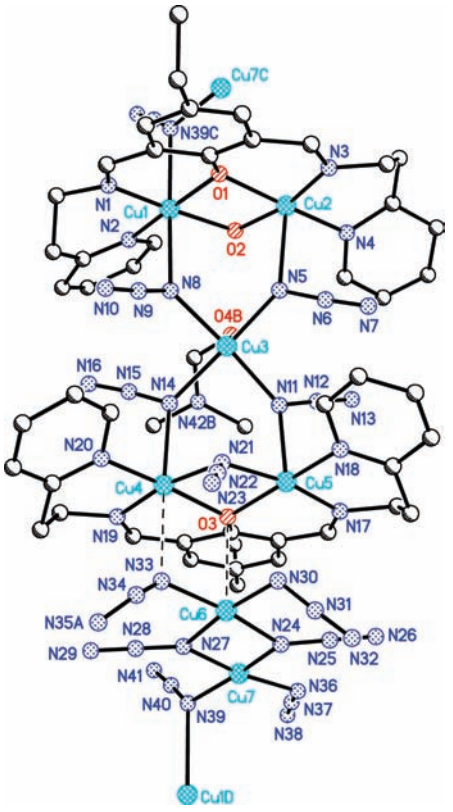

Figure 5. Perspective view of the structure of heptacopper(II)-based one-dimensional polymeric self-assembly $[\{Cu^{II}_2L(\mu\text{-}OH)\}\{Cu^{II}_2L(\mu_{1,1}\text{-}N_3)\}\{Cu^{II}(\mu_{1,1}\text{-}N_3)_4(dmf)\}\{Cu^{II}_2(\mu_{1,1}\text{-}N_3)_2(N_3)_4\}]_n\cdot n$dmf (**5**). Azide atoms N34 and N35 are disordered; hence, for clarity, only one component for each is shown. Symmetry codes: B, x, $y - 1$, z; C, $x - 1$, $y - 1$, $z - 1$; D, $1 + x$, $1 + y$, $1 + z$.

azide bridges to generate the tetracopper(II) moiety having three types of bridges, μ-phenoxo, $\mu_{1,1}$-N_3, and $\mu_{1,3}$-N_3. Cu2 is additionally coordinated to a perchlorate oxygen atom (O3). Clearly, Cu2 is hexacoordinated, while Cu1 is pentacoordinated. Interestingly, the tetranuclear cluster **4**, resulting because of the interlinking of two μ-phenoxo-$\mu_{1,1}$-azide dinuclear units by end-to-end azide bridges, is a new type of structure in the family containing numerous azide compounds of any metal ion.

Crystal structure of $[\{Cu^{II}_2L(\mu\text{-}OH)\}\{Cu^{II}_2L(\mu_{1,1}\text{-}N_3)\}\{Cu^{II}(\mu_{1,1}\text{-}N_3)_4(dmf)\}\{Cu^{II}_2(\mu_{1,1}\text{-}N_3)_2(N_3)_4\}]_n\cdot n$dmf (**5**) is shown in Figure 5. The structure reveals that compound **5** is a heptacopper(II)-based one-dimensional polymer. This compound contains two L^-, each of which incorporates two metal ions; Cu1 and Cu2 occupy two compartments of one L^-, while Cu4 and Cu5 occupy two compartments of another L^-. In addition to the bridging phenoxo oxygen atom of L^-, Cu1 and Cu2 are bridged by an exogeneous hydroxo oxygen atom, while Cu4 and Cu5 are bridged by a nitrogen atom of an end-on azide anion. Each of the four metal ions of the Cu1···Cu2 and Cu4···Cu5 units are bridged with another copper(II) ion, Cu3, by each of four end-on azide anions. Clearly, five copper(II) ions, Cu1, Cu2, Cu3, Cu4, and Cu5, are the members of a pentacopper(II) unit, generated because of coordinate bondings. The remaining two copper(II) ions, Cu6 and Cu7, are bridged by two end-on azide ligands. Each of these two copper(II) centers are also coordinated to two other azide anions. The coordinating nitrogen atom, N33, of one such azide anion, coordinated to Cu6, interacts weakly with Cu4. Clearly, although the Cu4···N33 interaction is weak, it may be considered that Cu4 and Cu6 are bridged by an end-on azide anion. The bridging phenoxo oxygen atom, O3, of the Cu4···Cu5 unit interacts weakly with Cu6, and hence Cu4 and Cu5 may be considered as bridged with Cu6 because of the O3···Cu6 semicoordination. Clearly, while coordinate bonds are responsible to generate a pentacopper(II) unit containing Cu1, Cu2, Cu3, Cu4 and Cu5, as well as a dicopper(II) unit containing Cu6 and Cu7, these pentanuclear and dinuclear units are self-assembled to result in a heptacopper(II) aggregate because of Cu4—N33 and Cu6—O3 interactions. As already mentioned, in addition to the two end-on azide bridges, Cu7 is coordinated to two other azide anions. The coordinating nitrogen atom, N39, of one such azide anion interacts with a copper(II) center, Cu1D, of a symmetry related neighboring heptacopper(II) unit. Clearly, one heptacopper(II) aggregate is interlinked with two neighboring such aggregates because of two such end-on azide bridges (Cu7 is bridged with Cu1D, and Cu1 is bridged with Cu7C) to generate a heptacopper(II)-based one-dimensional polymer, which propagates along the crystallographic b axis. Interestingly, the heptanuclear assembly as well as the heptanuclear-based one-dimensional aggregate in **5** is a new type of structure in the family containing numerous azide compounds of any metal ion.

The displacement of the metal center and average deviation of the constituent atoms from the corresponding least-squares basal plane and the ranges of the *transoid* angles, *cisoid* angles, bond lengths involving the basal atoms, bond lengths involving the apical atoms along with the coordination geometry, apical moiety(ies), apical atom(s), and τ values for the metal centers in **1**—**5** are compared in Table S1 of the Supporting Information, while the selected bond lengths and angles in the coordination

dx.doi.org/10.1021/ic200409d |*Inorg. Chem.* 2011, 50, 7540–7554

environment of the metal ions in **1**−**5** are listed in Tables S2−S6 of the Supporting Information, respectively. The coordination geometry of the pentacoordinated metal ions, Cu1 and Cu2 in both **1** and **3**, Cu2 in **2**, Cu1 in **4**, and Cu2, Cu3, Cu5, and Cu6 in **5**, are square pyramidal. On the other hand, the coordination geometry of the hexacoordinated metal centers, Cu1 in **2**, Cu2 in **4**, and Cu1 and Cu4 in **5**, is distorted octahedral. The only tetracoordinated metal ion, Cu7 in **5**, adopts a distorted square planar coordination geometry. Varying extent of distortion of the coordination environments is evidenced by the τ values (0.043−0.35), average deviation (0.003−0.30 Å) of the constituent atoms, and displacement (0.008−0.27 Å) of the metal ions from the corresponding least-squares basal plane. As listed in Table S1 of the Supporting Information, the ranges of the *cisoid* and *transoid* angles, along with the ranges of the bond lengths are also indicative of varying extent of distortion. As usual for copper(II), the bond distance(s) involving the apical atom(s) is/are significantly longer than the bond distances involving the basal atoms for all the metal centers in **1**−**5**.

For all the pairs of metal ions interlinked by bridging ligands in **1**−**5**, the bridging moiety, bridging fashion (equatorial−equatorial, axial−axial, or equatorial−axial), the metal···metal distance, bridge angle(s), and dihedral angle (δ) between the two basal planes are summarized in Table 2. These aspects are described below along with the description of magnetic properties.

Magnetic Properties of 1−4. The cryomagnetic behavior of $[Cu^{II}_2L(\mu_{1,1}\text{-}NO_3)(H_2O)(NO_3)](NO_3)$ (**1**), $[\{Cu^{II}_2L(\mu\text{-}OH)(H_2O)\}(\mu\text{-}ClO_4)]_n(ClO_4)_n$ (**2**), $[\{Cu^{II}_2L(NCS)_2\}(\mu_{1,3}\text{-}NCS)]_n$ (**3**), and $[\{Cu^{II}_2L(\mu_{1,1}\text{-}N_3)(ClO_4)\}_2(\mu_{1,3}\text{-}N_3)_2]$ (**4**) are shown as χT versus T plots in Figure 6, Figures S2 and S3 of the Supporting Information, and Figure 7, respectively. The χT values at 300 K for **1**−**4** are 0.57, 0.15, 0.62, and 1.00 cm^3 $K\,mol^{-1}$, respectively, which are smaller than the expected values of 0.75 cm^3 $K\,mol^{-1}$ for two copper(II) ions (for **1**−**3**) and 1.5 cm^3 $K\,mol^{-1}$ for four copper(II) ions (for **4**) with $g = 2.0$ and $S = 1/2$. As the χT value of complex **2** is only 0.15 cm^3 $K\,mol^{-1}$ at 300 K, susceptibility data of this compound were collected for higher temperatures up to 370 K. However, the χT value at 370 K is also significantly smaller, 0.26 cm^3 $K\,mol^{-1}$. As temperature decreases from 370 K for **2** and from 300 K for **1**, **3**, and **4**, the χT product decreases steadily until the samples become diamagnetic below 100 K for complex **1**, 200 K for **2**, and 50 K for compounds **3** and **4**. The susceptibility data indicate very strong antiferromagnetic interaction in **2** and strong antiferromagnetic interaction in **1**, **3**, and **4**.

As compound **1** is an isolated dicopper(II) system, the magnetic data of **1** were modeled with the spin Hamiltonian $\hat{H} = -2J[\hat{S}_1 \cdot \hat{S}_2]$. In compounds **2**, **3**, and **4**, the magnetic exchange between the μ-phenoxo-μ-hydroxo dicopper(II) (in **2**), μ-phenoxo dicopper(II) (in **3**), and μ-phenoxo-$\mu_{1,1}$-azide dicopper(II) (in **4**) units should be very weak because of the occupation of the bridging perchlorate oxygen atoms (in **2**), end-to-end thiocyanate nitrogen and sulfur atoms (in **3**), and end-to-end azide nitrogen atoms (in **4**) in the axial positions (axial−axial) as well as because of long copper(II)−perchlorate (2.683(5) and 2.536 (9) Å), copper(II)−$\mu_{1,3}$-thiocyanate (2.190(2) and 2.7936(8) Å), and copper(II)−$\mu_{1,3}$-azide (2.2370(19) and 2.5786(17) Å) bond distances (Tables 2, S1, and S3−S5 of the Supporting Information). On the other hand, as is discussed below, μ-phenoxo-μ-hydroxo, μ-phenoxo, and μ-phenoxo-$\mu_{1,1}$-azide moieties in **2**, **3**, and **4**, respectively, offer a very good pathway of strong or very strong antiferromagnetic coupling between the metal centers in the dinuclear unit. Clearly, in comparison to the strong or very strong interaction within the dinuclear unit, the very weak interaction through the axial−axial bridging perchlorate, thiocyanate and azide moieties can be logically neglected, and therefore, the magnetic data of compounds **2**, **3**, and **4** were modeled as isolated dicopper(II) systems, using the same spin Hamiltonian as that of compound **1**. In the susceptibility versus T plot of **3**, one can observe an increase at the lowest temperatures, after a maximum is reached, which indicates the presence of a small amount of paramagnetic impurity (ρ). Fitting of the experimental data with the theoretical expression results in $J = -135$ cm^{-1} and $g = 2.19$ for **1**, $J = -298$ cm^{-1} and $g = 2.14$ for **2**, $J = -105$ cm^{-1}, $g = 2.24$, and $\rho = 5\%$ for **3**, and $J = -119.5$ cm^{-1} and $g = 2.07$ for **4**.

In addition to some relevant structural informations, the J values of **1**−**4** are listed in Table 2. The magnetic orbital for all the copper(II) centers in **1**−**4** is $dx^2 - y^2$. In **2**, both the bridging oxygen atoms, phenoxo and hydroxo, occupy basal positions (equatorial−equatorial) of both of the metal centers with bridge angles, 100.81(17)° and 105.25(17)°, respectively, greater than the crossover angle (97.5°).[1a,8] Moreover, the bridging moiety is nearly planar as evidenced by the torsion angle (7.7°) in the $[Cu_2O_2]$ unit and the dihedral angle (δ = 13.7°) between the two basal planes. All these structural parameters[1a,8,9] indicate propagation of very strong antiferromagnetic interaction, as observed ($J = -298$ cm^{-1}) in **2**. In **1**, while the bridging phenoxo oxygen atom occupies basal positions (equatorial−equatorial) for both the metal ions with the bridge angle of 107.19(13)°, the bridging nitrate oxygen atom occupies the basal position for one metal ion and the axial position for the second (axial−equatorial) with the bridge angle of 95.50(11)°. Clearly, the nitrate route can only mediate weak interaction and that may be ferromagnetic, eventually reducing the overall strength of antiferromagnetic coupling that is expected through the phenoxo pathway. The extent of antiferromagnetic interaction is further reduced due to twisting of the bridging moiety, as evidenced by the torsion angle (23°) in the $[Cu_2O_2]$ unit and the dihedral angle (δ = 40.4°) between the two basal planes. Eventually, the magnitude of antiferromagnetic coupling constant of **1** (−135 cm^{-1}) is much smaller than that of **2** (−298 cm^{-1}). The phenoxo oxygen bridges two metal ions in **3** in equatorial−equatorial fashion. As the Cu−O−Cu bridge angle in **3** is 110° greater than those (95.5 and 107.2° in **1**; 100.8 and 105.2° in **2**) in **1** and **2**, one would expect stronger antiferromagnetic interaction in the former. However, as the bridging moiety in **3** is more twisted than those in **1** and **2** (δ = 40.4, 13.7, and 52.9° in **1**, **2** and **3**, respectively), antiferromagnetic interaction in **3** ($J = -105$ cm^{-1}) becomes weaker than those in **1** and **2**.[1a,8−10] The magnetic interaction through the heterobridged μ-phenoxo-$\mu_{1,1}$-azide moiety[4,5,9f] (both bridges are equatorial−equatorial) is a combined effect of the superexchange through the two individual bridges, phenoxo and end-on azide. As the phenoxo bridge angle (102°) is greater than 97.5°, antiferromagnetic interaction is expected. On the other hand, as the end-on azide bridge angle (101°) is less than 108°, the azide route should propagate ferromagnetic interaction.[6] Superexchange through the phenoxo route dominates over that through the end-on azide route resulting in $J = -119.5$ cm^{-1}.

It is relevant to mention the magnetic exchange interaction in the previously reported related compounds. In a few μ-phenoxo-μ-hydroxo dicopper(II) complexes, characterized by both single crystal structures and magnetic studies, both the bridges are equatorial−equatorial (as in **2**) with bridge angles greater than

Table 2. *J* Values/Expected Magnetic Interaction along with Some of Structural Information that may Influence Magnetic Properties

compound	bridged metal pair	bridging moiety	bridging fashion	bridge angle (deg)	metal···metal mistance (Å)	δ (deg)	J (cm^{-1})/ expected interaction
1	Cu1···Cu2	μ-phenoxo	phenoxo: eq(Cu1)-eq(Cu2)	Cu1−O1−Cu2 = 107.19(13)	3.1969(14)	40.4	−135
		$\mu_{1,1}$-NO_3	$\mu_{1,1}$-NO_3: ax(Cu1)-eq(Cu2)	Cu1−O2−Cu2 = 95.50(11)			
2	Cu1···Cu2	μ-phenoxo	phenoxo: eq(Cu1)-eq(Cu2)	Cu1−O1−Cu2 = 100.81(17)	3.0519(9)	13.7	−298
		μ-hydroxo	hydroxo: eq(Cu1)-eq(Cu2)	Cu1−O2−Cu2 = 105.25(17)			
	Cu1···Cu1D	μ-ClO_4	μ-ClO_4: ax(Cu1)-ax(Cu1D)		7.2791(3)	7.9	negligible
3	Cu1···Cu2	μ-phenoxo	phenoxo: eq(Cu1)-eq(Cu2)	Cu1−O1−Cu2 = 110.13(8)	3.2553(4)	52.9	−105
	Cu1···Cu2A	$\mu_{1,3}$-SCN	$\mu_{1,3}$-SCN: ax(Cu1)-ax(Cu2A)		6.0234(5)	52.9	negligible
4	Cu1···Cu2	μ-phenoxo	phenoxo: eq(Cu1)-eq(Cu2)	Cu1−O1−Cu2 = 102.36(6)	3.0970(3)	23.1	−119.5
		$\mu_{1,1}$-azide	$\mu_{1,1}$-azide: eq(Cu1)-eq(Cu2)	Cu1−N5−Cu2 = 101.39(8)			
	Cu1···Cu2A	$\mu_{1,3}$-azide	$\mu_{1,1}$-azide: ax(Cu1)-ax(Cu2A)		6.0148(4)	23.1	negligible
5	Cu1···Cu2	μ-phenoxo	phenoxo: eq(Cu1)-eq(Cu2)	Cu1−O1−Cu2 = 98.3(3)	3.0398(19)	5.0	antiferromagnetic
		μ-hydroxo	hydroxo: eq(Cu1)-eq(Cu2)	Cu1−O2−Cu2 = 103.5(3)			
	Cu4···Cu5	μ-phenoxo	phenoxo: eq(Cu4)-eq(Cu5)	Cu4−O3−Cu5 = 98.8(3)	3.0522(18)	6.1	antiferromagnetic
		$\mu_{1,1}$-azide	$\mu_{1,1}$-azide: eq(Cu4)-eq(Cu5)	Cu4−N21−Cu5 = 103.6(4)			
	Cu6···Cu7	$\mu_{1,1}$-azide	$\mu_{1,1}$-azide: eq(Cu6)-eq(Cu7)	Cu6−N24−Cu7 = 104.3(5)	3.1294	6.1	ferromagnetic
		$\mu_{1,1}$-azide	$\mu_{1,1}$-azide: eq(Cu6)-eq(Cu7)	Cu6−N27−Cu7 = 102.9(5)			
	Cu1···Cu3	$\mu_{1,1}$-azide	$\mu_{1,1}$-azide: ax(Cu1)-eq(Cu3)	Cu1−N8−Cu3 = 124.3(4)	4.016(2)	55.0	weak ferromagnetic
	Cu2···Cu3	$\mu_{1,1}$-azide	$\mu_{1,1}$-azide: ax(Cu2)-eq(Cu3)	Cu2−N5−Cu3 = 127.2(4)	3.946(2)	52.2	weak ferromagnetic
	Cu3···Cu4	$\mu_{1,1}$-azide	$\mu_{1,1}$-azide: eq(Cu3)-ax(Cu4)	Cu3−N14−Cu4 = 127.8(5)	3.948(2)	48.7	weak ferromagnetic
	Cu3···Cu5	$\mu_{1,1}$-azide	$\mu_{1,1}$-azide: eq(Cu3)-ax(Cu5)	Cu3−N11−Cu5 = 129.1(5)	3.880(2)	47.9	weak ferromagnetic
	Cu1···Cu7C	$\mu_{1,1}$-azide	$\mu_{1,1}$-azide: ax(Cu1)-eq(Cu7C)	Cu1−N39C−Cu7C = 99.3(4)	3.3803(18)	7.9	weak ferromagnetic
	Cu4···Cu6	μ-phenoxo	phenoxo: eq(Cu4)-ax(Cu6)	Cu4−O3−Cu6 = 94.1(3)	3.5062(17)	5.0	weak ferromagnetic
		$\mu_{1,1}$-azide	$\mu_{1,1}$-azide: ax(Cu4)-eq(Cu6)	Cu4−N33−Cu6 = 95.2(6)			
	Cu5···Cu6	μ-phenoxo	phenoxo: eq(Cu5)-ax(Cu6)	Cu5−O3−Cu6 = 94.8(3)	3.5293(18)	7.6	weak ferromagnetic

the crossover angle (97.5°), and the J values in these compounds range between −182 and −426 cm^{-1}.[9] Previously reported monophenoxo-bridged dicopper(II) compounds having the equatorial−equatorial bridging fashion as in **3** are coupled by moderate antiferromagnetic interaction with J values lying between −48 and −122 cm^{-1}.[10] As in **4**, the antiferromagnetic phenoxo route dominates over the ferromagnetic azide route in all of the previously reported μ-phenoxo-$\mu_{1,1}$-azide compounds,[4,5,9f] resulting in weak[5c] (e.g., J = −8.7 cm^{-1}), moderate[4d] (e.g., J = −43.2 cm^{-1}), strong[5b] (e.g., J = −119 cm^{-1}), and very strong[4a] (e.g., J = −204 cm^{-1}) antiferromagnetic interaction. Although compound **1** has a new bridging moiety, its magnetic behavior could be rationalized on the basis of established magnetostructural correlation.

Magnetic Properties of 5. DC magnetic susceptibility data were collected for a crushed crystalline sample of $[\{Cu^{II}_2L(\mu\text{-}OH)\}\{Cu^{II}_2L(\mu_{1,1}\text{-}N_3)\}\{Cu^{II}(\mu_{1,1}\text{-}N_3)_4(dmf)\}\{Cu^{II}_2(\mu_{1,1}\text{-}N_3)_2(N_3)_4\}]_n\cdot n$dmf (**5**) at an applied magnetic field of 1 T in the 2−300 K temperature range and 300 G in the 2−30 K temperature range. No field dependence of the magnetic susceptibility response was observed. The data are shown in Figure 8 as a χT versus T plot. The χT value at 300 K is 2.4 cm^3 K mol^{-1}, below than the expected value of 2.6 cm^3 K mol^{-1} for seven Cu(II) ions with g = 2.0 and S = 1/2. As temperature decreases,

dx.doi.org/10.1021/ic200409d |*Inorg. Chem.* 2011, 50, 7540–7554

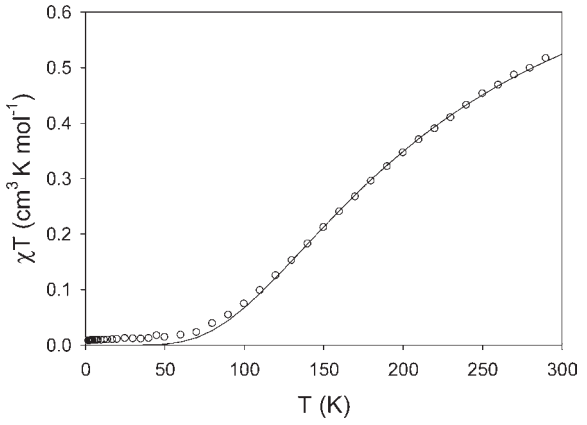

Figure 6. χT vs T plot of $[Cu^{II}_2L(\mu_{1,1}\text{-}NO_3)(H_2O)(NO_3)](NO_3)$ (**1**). The solid line is the best fitting to the experimental data.

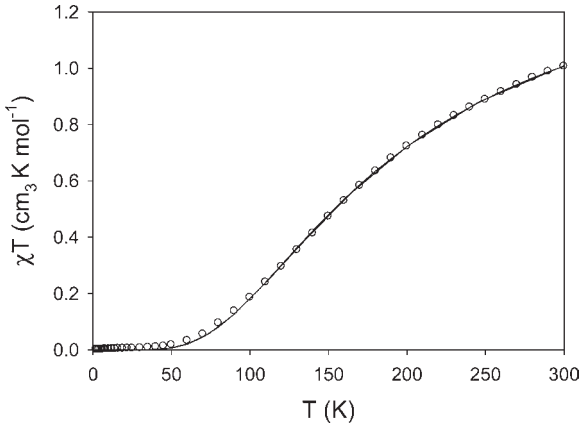

Figure 7. χT vs T plot of $[\{Cu^{II}_2L(\mu_{1,1}\text{-}N_3)(ClO_4)\}_2(\mu_{1,3}\text{-}N_3)_2]$ (**4**). The solid line is the best fitting to the experimental data.

the χT product decreases until a plateau is reached at 80 K, with a χT product value of 1.5 cm^3 K mol^{-1}. This indicates a combination of antiferromagnetic and ferromagnetic pairwise interactions between the seven Cu(II) ions that lead to a nonzero ground state. In fact, the plateau in the χT versus T plot suggests an $S_T = 3/2$ for each $[Cu_7]$ unit that form the coordination polymer **5**. This is further confirmed by the magnetization versus field measurement at 2 K; as shown in Figure 9, the magnetization tends to saturation at a value of 3, indicating $S_T = 3/2$ spin ground state. The solid line is the Brillouin function for $g = 2.1$ and $S_T = 3/2$. The lack of agreement observed in the midfield range is caused by the existence of low lying excited states because the $S = 3/2$ is not an isolated state due to the fact that complex **5** is a polymer of weakly coupled $S = 3/2$ units.

Complex **5** is a coordination polymer formed by repeating $[Cu_7]$ units (Figures 5 and 10). Even though **5** is too complicated to model the magnetic data, the pairwise interactions can be qualitatively evaluated (Figure 10 and Table 2) thanks to the extensive magnetostructural correlations and calculations performed on dicopper(II) complexes with hydroxo,[1a] phenoxo[1a,8] or end-on N_3[3d,6] bridges, as those found in **5**. The magnetic orbital of all the copper(II) centers in **5** is $dx^2 - y^2$. The metal centers in the Cu1···Cu2 unit are bridged by a μ-phenoxo-μ-hydroxo moiety where both the bridges are equatorial−equatorial with

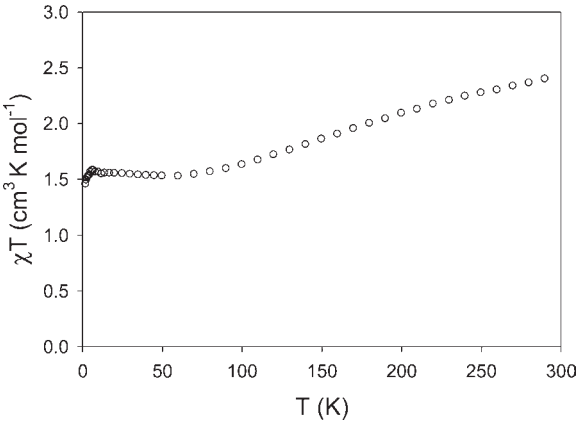

Figure 8. χT vs T plot of $[\{Cu^{II}_2L[\{Cu^{II}_2L(\mu\text{-}OH)\}\{Cu^{II}_2L(\mu_{1,1}\text{-}N_3)\}\text{-}\{Cu^{II}(\mu_{1,1}\text{-}N_3)_4(dmf)\}\{Cu^{II}_2(\mu_{1,1}\text{-}N_3)_2(N_3)_4\}]_n \cdot n$dmf (**5**) at 1 T from 2 to 300 K and 300 G from 2 to 30 K.

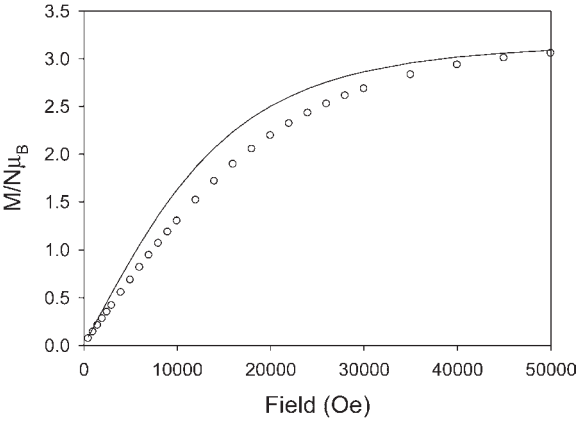

Figure 9. Magnetization versus field plot for $[\{Cu^{II}_2L(\mu\text{-}OH)\}\{Cu^{II}_2L\text{-}(\mu_{1,1}\text{-}N_3)\}\{Cu^{II}(\mu_{1,1}\text{-}N_3)_4(dmf)\}\{Cu^{II}_2(\mu_{1,1}\text{-}N_3)_2(N_3)_4\}]_n \cdot n$dmf (**5**) at 2 K. The solid line is the best Brillouin function for $S = 3/2$ and $g = 2.1$.

Cu−O−Cu angles of 103.5° and 98.3°, and therefore, Cu1 and Cu2 should be coupled antiferromagnetically. The metal centers in the Cu4···Cu5 pair are bridged by a μ-phenoxo-$\mu_{1,1}$-azide moiety, and both the bridges coordinate in equatorial−equatorial fashion. The Cu−O−Cu and Cu−N−Cu angles are 98.8° and 103.6°; thus, weak antiferromagnetic coupling is expected. The Cu6···Cu7 unit is bridged by two end-on azido ligands with Cu−N−Cu angles of 102.9° and 104.3°, which as calculated by Alvarez et al[3d] should lead to ferromagnetic coupling. The bridging moieties in the Cu1···Cu7C, Cu4···Cu6, and Cu5···Cu6 are, respectively, $\mu_{1,1}$-azide, μ-phenoxo-$\mu_{1,1}$-azide, and μ-phenoxo. As all these bridges coordinate in axial−equatorial fashion, weak ferromagnetic interaction is expected between the metal ions in these three pairs. Finally, Cu3 is bridged to Cu1, Cu2, Cu4, and Cu5 by four end-on azido ligands, all of which are equatorial−axial. The interaction between Cu3 and its four neighbors will thus be very weak ferromagnetic, which is frustrated due to the dominant antiferromagnetic coupling within the Cu1···Cu2 and Cu4···Cu5 pairs. Thus, five Cu(II) ions in **5** have their spins parallel to the magnetic field, while the other two align theirs an antiparallel fashion (Figure 10) resulting in the

dx.doi.org/10.1021/ic200409d |*Inorg. Chem.* 2011, 50, 7540–7554

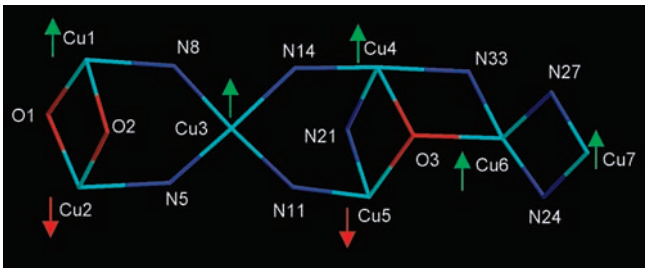

Figure 10. Core of the $[Cu_7]$ repeating unit of Complex **5**, with a schematic representation of the spin alignments in the complex.

Table 3. UV−Vis Spectral Bands in dmf along with Tentative Assignment

compounds	λ_{nm} (ε, M^{-1} cm^{-1})	tentative assignment
1	267 (34287)	$\pi \rightarrow \pi^*$
	374 (8680)	$PhO^-/NO_3^- \rightarrow$ Cu(II)
	648 (145)	d → d
2	267 (33980)	$\pi \rightarrow \pi^*$
	384(7360)	$PhO^-/OH^- \rightarrow$ Cu(II)
	635 (130)	d → d
3	266 (34305)	$\pi \rightarrow \pi^*$
	368 (6280)	$PhO^-/NCS^- \rightarrow$ Cu(II)
	660 (154)	d → d
4	267 (33567)	$\pi \rightarrow \pi^*$
	384 (15600)	$PhO^-/N_3^- \rightarrow$ Cu(II)
	713 (390)	d → d
5	267 (33960)	$\pi \rightarrow \pi^*$
	380 (17800)	$PhO^-/OH^-/N_3^- \rightarrow$ Cu(II)
	707 (634)	d → d

observed experimental value of $S_T = 3/2$ for the repeating $[Cu_7]$ unit of **5**.

Electronic Spectra and Catecholase Activity. All the complexes **1**−**5** are practically insoluble in methanol but well soluble in dmf. Again, while compounds **1**, **2**, and **4** are soluble in acetonitrile, other two compounds (**3** and **5**) are practically insoluble in acetonitrile. Accordingly, electronic spectra (200−1200 nm) of **1**, **2**, and **4** were recorded in both MeCN and dmf, while those of **3** and **5** were recorded in dmf only. The band positions and ε values in dmf are listed in Table 3. In dmf, three characteristic bands are observed in all the spectra: two strongly intense bands at 266/267 nm (ε about 34000 M^{-1} cm^{-1}) and in the range of 368−384 nm (ε = 6280−17800 M^{-1} cm^{-1}) and a less intensity band in the range of 635−713 nm (ε = 130−634 M^{-1} cm^{-1}). The spectra of **1**, **2**, and **4** in MeCN are almost similar to those in dmf, except that band intensity and position of band maximum are slightly changed. The probable assignment of the bands is summarized in Table 3.

3,5-Di-*tert*-butylcatechol (3,5-DTBCH$_2$) is usually used to study the catecholase activity of copper(II) complexes because of the ease of oxidation of 3,5-DTBCH$_2$ to its corresponding quinone, 3,5-di-*tert*-butylquinone (3,5-DTBQ), the later of which has a characteristic transition at about 400 nm.[5b,13a−13c,14b−14f,15−21] To check the ability of complexes **1**−**5** to behave as catalysts for catecholase activity, a 0.25 × 10^{-4} M solution of a complex is treated with a 100-fold concentrated solution of 3,5-DTBCH$_2$, and the course of the reaction was followed by recording UV−vis spectra of the mixture under aerobic condition at different times up to 60 or 90 min. Experiments with complexes **1**, **2**, and **4** were done in both MeCN and dmf to check the role of solvent on the catalytic activity, while the experiments with complexes **3** and **5** were done in dmf only because these two complexes are practically insoluble in MeCN.

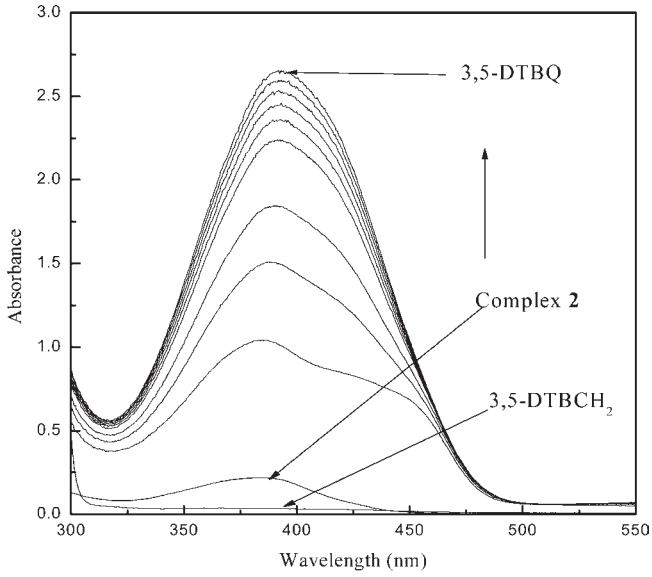

Figure 11. Spectral profile showing the increase of quinone band at 393 nm after the addition of 100 fold of 3,5-DTBCH$_2$ to a solution containing complex **2** (0.25 × 10^{-4} M) in MeCN. Spectra were recorded after each 5 min.

Spectral changes of complex **2** in MeCN are shown in Figure 11. After mixing 3,5-DTBCH$_2$ with complex **2**, the spectral changes at an interval of 5 min are shown in this figure. Because of the addition of 3,5-DTBCH$_2$, the LMCT band of the complex **2** at 384 nm becomes slightly red-shifted to 393 nm with gradual increase of intensity, indicating more and more formation of the quinone, 3,5-DTBQ. Clearly, complex **2** in acetonitrile shows catecholase activity. Similar spectral changes take place for complex **2** in dmf (Figure S4 of the Supporting Information), for complex **4** in MeCN (Figure S5 of the Supporting Information) and dmf (Figure 12), and for complex **5** in dmf (Figure S6 of the Supporting Information). On the other hand, generation of the quinone band does not take place for complex **1** in both MeCN and dmf and for complex **3** in dmf. Clearly, complexes **1** and **3** are not catalysts of catecholase activity. On the other hand, complexes **2** and **4** in both MeCN and dmf and complex **5** in dmf show catecholase activity. At this juncture, it may be mentioned that the maximum of the quinone band changes slightly as the function of a particular complex as well as of the solvent: 393 nm for **2** in MeCN, 393 nm for **2** in dmf, 397 nm for **4** in MeCN, 393 nm for **4** in dmf, and 395 nm for **5** in dmf.

Kinetic studies of the catecholase activity of catalyst complexes **2**, **4**, and **5** have been performed to understand the extent of their efficiency. For this purpose, a 0.25 × 10^{-4} M solution of a complex was treated with the substrate solution having concentration ranging between 10-fold and 100-fold than that of the complex. The experiments were done at a constant temperature, 25 °C, under aerobic condition. For a particular complex−substrate mixture, time scan at the maximum of the quinone band was carried out for a period of 60−90 min. It may be noted here

dx.doi.org/10.1021/ic200409d |*Inorg. Chem.* 2011, 50, 7540–7554

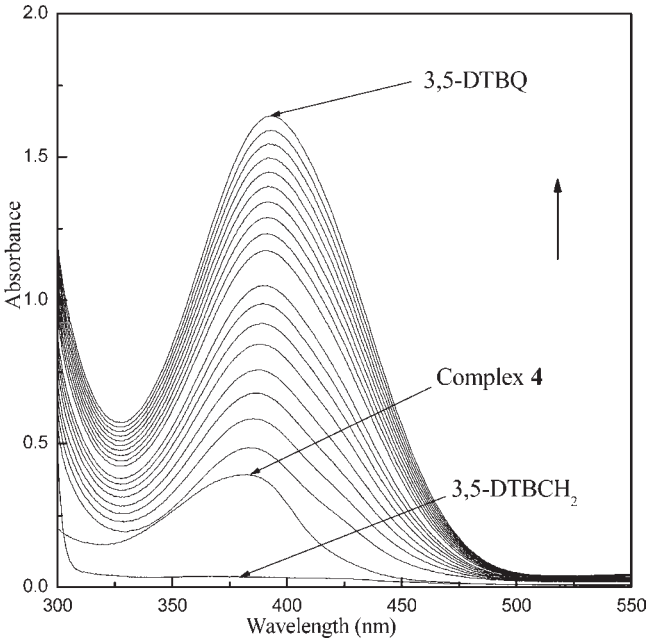

Figure 12. Spectral profile showing the increase of quinone band at 393 nm after the addition of 100 fold of 3,5-DTBCH$_2$ to a solution containing complex **4** (0.25×10^{-4} M) in dmf. Spectra were recorded after each 5 min.

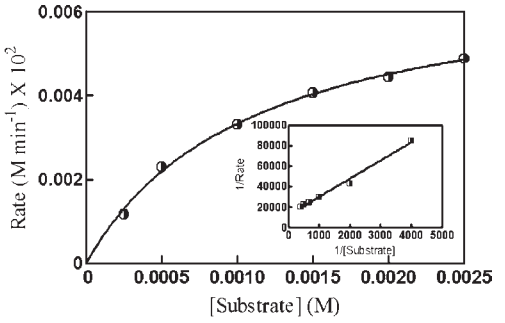

Figure 13. Initial rates versus substrate concentration for the 3,5-DTBCH$_2$ → 3,5-DTBQ oxidation reaction catalyzed by complex **2** in acetonitrile. Inset shows Lineweaver–Burk plot. Symbols and solid lines represent the observed and simulated profiles, respectively.

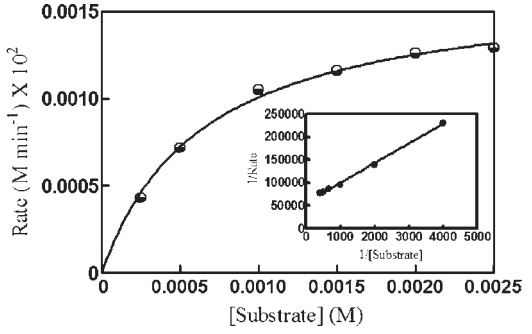

Figure 14. Initial rates versus substrate concentration for the 3,5-DTBCH$_2$ → 3,5-DTBQ oxidation reaction catalyzed by complex **4** in dmf. Inset shows Lineweaver–Burk plot. Symbols and solid lines represent the observed and simulated profiles, respectively.

that the blank experiment without a catalyst does not show formation of the quinone up to 12 h in MeCN and up to 3 h in dmf. The rate constant for a particular complex–substrate mixture was determined from the optical density versus time plot by the initial rate method. The rate constant versus concentration of substrate data were then analyzed on the basis of the Michaelis–Menten approach of enzymatic kinetics to get the Lineweaver–Burk plot as well as the values of the parameters V_{max}, K_M, and K_{cat}. Observed and simulated rate constant versus [substrate] plots and the Lineweaver–Burk plot for complex **2** in MeCN and complex **4** in dmf are shown in Figures 13 and 14, respectively, while similar plots for complex **2** in dmf, for complex **4** in MeCN, and complex **5** in dmf are shown in Figures S7, S8, and S9 of the Supporting Information, respectively. The kinetic parameters for all the cases are listed in Table 4. Compounds **2**, **4**, and **5** show turnover numbers (K_{cat}) in between 39 and 215 h^{-1}, which lie in the range of the K_{cat} values of other model complexes, and therefore, the compounds **2**, **4**, and **5** can be considered as functional models of catechol oxidase.[5b,13a−13c,14b−14f,15−21] The better efficiency in MeCN in comparison to dmf probably occurs because dmf is a better coordinating solvent.

The native met form of catechol oxidase consists of a hydroxo-bridged dicopper(II) center. On the other hand, all the model copper(II) compounds showing catecholase activity are either dicopper(II) or monocopper(II). Interestingly, only in the present investigation, a cluster (**4**) or one-dimensional copper(II) compounds (**2** and **5**), have been checked for the first time to show catecholase activity and also found as active catalyst.

It has been proposed previously that several factors may influence the efficiency of a complex to catalyze catecholase activity.[5b,9d,13,14,19,20] These factors are Cu···Cu distance, coordination geometry around the metal center, nature of the exogeneous bridging ligand, flexibity of the primary ligand, etc. However, a literature survey reveals that the problem is rather complicated. For example, while a Cu···Cu distance in the range of 2.9–3.25 Å is proposed as the optimum for best catalyst,[13b,14e,19] a number of good catalysts are known in which this distance lies at about 4 Å and even much larger such as 7.8 Å.[13b] Again, there is example of poor activity in spite of Cu···Cu distance, 2.85 Å, less than even 2.9 Å.[14b] Similar complications are there regarding coordination geometry.[9d,14a−14c,14g,14h] In the crystal structure of the met form of the enzyme, two copper(II) centers are hydroxo-bridged, and each is a trigonal pyramidal. In model systems, some authors observed and proposed better activity if the coordination geometry is a trigonal bipyramidal,[14c] while some others observed better activity for square pyramidal[14a] or even square planar[14g,14h], cases. Regarding the exogeneous bridging ligand, it has been proposed that activity should be better for small exogeneous ligands, hydroxo for example.[5b,14e,14f,15b] In practice, although some hydroxo-bridged complexes are known as efficient catalysts, some other are also known with very poor activity. Clearly, the ability of a complex to show catecholase activity as well as the turn over number is a composite effect of several parameters. Nonetheless, some comments may be noted regarding the activity of the title compounds. The lack of activity for the μ-phenoxo-$\mu_{1,1}$-nitrate dicopper(II) compound **1** may be due to the fact that nitrate is a poor leaving group and the catechol moiety cannot substitute it. In contrast, the hydroxo group in **2**, end-on azide in **4**, and either or both of the hydroxo and end-on azide in **5** are the leaving groups in

dx.doi.org/10.1021/ic200409d |*Inorg. Chem.* 2011, 50, 7540–7554

Table 4. Kinetic Parameters for the Complexes

complex	solvent	V_{max} (M min^{-1})	std. error	K_M (M)	std. error	K_{cat} (h^{-1})
2	dmf	1.628×10^{-5}	1.592×10^{-6}	0.000686	0.0002103	39.0
	acetonitrile	6.996×10^{-5}	2.791×10^{-6}	0.001096	0.0001029	167.9
4	dmf	1.662×10^{-5}	4.917×10^{-7}	0.000651	0.0000571	39.9
	acetonitrile	8.606×10^{-5}	4.682×10^{-6}	0.001304	0.0001549	215.1
5	dmf	2.007×10^{-5}	9.344×10^{-7}	0.000436	0.0000724	48.2

presence of catechol moiety to result in the catecholase activity of these three complexes.

It is also relevant to mention the activity of previously published systems having bridging moieties, closely similar to those in the title compounds. Activity of a few dicopper(II) compounds having μ-phenoxo-μ-hydroxo moiety has been checked; while some are inactive, most are active with K_{cat} values ranging between 5 and 5470 h^{-1}.[9d,13a−13c,14] Out of four monophenoxo-bridged dicopper(II) compounds for which activity has been tested, two are inactive, while two others are active with K_{cat} values 37 and 900 h^{-1}.[21] On the other hand, very low catalytic activity has been observed for a μ-phenoxo-μ-hydroxo-μ-perchlorate dicopper(II) compound derived from 2,6-bis[N-(2-pyridylethyl)-formidoyl]-4-methylphenol.[22] The low activity in this case probably arises because of the triple-bridging moiety, which imposes a steric limitation of the catechol to coordinate to the metal ion.

Electrospray Ionization Mass Spectral Study. The electrospray ionization mass spectroscopy (ESI-MS positive) spectra of compounds **1**, **2**, and **4** were recorded in acetonitrile solutions. The spectra of $[Cu^{II}_2L(\mu_{1,1}\text{-}NO_3)(H_2O)(NO_3)](NO_3)$ (**1**), $[\{Cu^{II}_2L(\mu\text{-}OH)(H_2O)\}(\mu\text{-}ClO_4)]_n(ClO_4)_n$ (**2**) and $[\{Cu^{II}_2L(\mu_{1,1}\text{-}N_3)(ClO_4)\}_2(\mu_{1,3}\text{-}N_3)_2]$ (**4**) are shown in Figure S10 of the Supporting Information, Figure 15, and Figure S11 of the Supporting Information, respectively.

Compound **2** exhibits four peaks at m/z = 264 (100%, line to line separation 0.5), 345 (13%, line to line separation 1.0), 529 (25%, line to line separation 1.0), and 628 (38%, line to line separation 1.0). The peaks at m/z = 264 and 628 are well assignable to the μ-phenoxo-μ-hydroxo dicopper(II) species, dicationic $[Cu^{II}_2L(\mu\text{-}OH)]^{2+}$ ($C_{24}H_{26}N_4O_2Cu_2$) and monocationic $[Cu^{II}_2L(\mu\text{-}OH)(ClO_4)]^+$ ($C_{24}H_{26}N_4O_6ClCu_2$), respectively, while the peak at 529 can be assigned to the monocationic dinuclear μ-phenoxo-μ-oxo moiety $[Cu^{II}_2L(\mu\text{-}O)]^+$ ($C_{24}H_{25}N_4O_2Cu_2$). On the other hand, the observation of the peak at 345 indicates the presence of the mononuclear monocationic species $[Cu^{II}L^1]^+$ ($C_{17}H_{17}N_2O_2Cu$); HL^1 is the 1:1 condensation product of 2,6-diformyl-4-ethylphenol and 2-(2-aminoethyl)pyridine. As shown in Figure 15, the isotopic distribution of the observed and simulated spectral patterns are in excellent agreement with each other, indicating right assignment of the positive ions.

The ESI-MS positive spectrum of compound **4** (Figure S11 of the Supporting Information) is similar to that of compound **2**. The spectrum of compound **1** (Figure S10 of the Supporting Information) is also similar to that of complexes **2** and **4**, except that the peak at m/z 628 due to $[Cu^{II}_2L(\mu\text{−}OH)(ClO_4)]^+$ is not present because compound **1** does not contain a perchlorate moiety.

Compound **2**, $[\{Cu^{II}_2L(\mu\text{-}OH)(H_2O)\}(\mu\text{-}ClO_4)]_n(ClO_4)_n$, contains a μ-phenoxo-μ-hydroxo dicopper(II) core, and therefore,

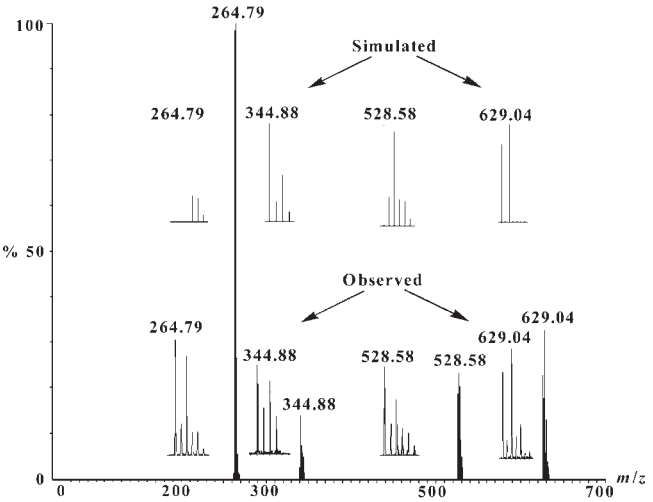

Figure 15. Electrospray mass spectrum (ESI-MS positive) of $[\{Cu^{II}_2L(\mu\text{-}OH)(H_2O)\}(\mu\text{-}ClO_4)]_n(ClO^4)_n$ (**2**) in acetonitrile showing observed and simulated isotopic distribution pattern.

the observation of positive ions $[Cu^{II}_2L(\mu\text{-}OH)]^{2+}$ and $[Cu^{II}_2L(\mu\text{-}OH)(ClO_4)]^+$, both having a μ-phenoxo-μ-hydroxo dicopper(II) core, is quite normal. However, the appearance of a positiove ion $[Cu^{II}_2L(\mu\text{-}O)]^+$ having a μ-phenoxo-μ-oxo dicopper(II) core is interesting. Again, significant decomposition of the ligand system takes place to stabilize a mononuclear positive ion $[Cu^{II}L^1]^+$, which contains a ligand having one formyl group condensed with the amine moiety but the second formyl group remaining as such.

$[\{Cu^{II}_2L(\mu_{1,1}\text{-}N_3)(ClO_4)\}_2(\mu_{1,3}\text{-}N_3)_2]$ (**4**) and $[Cu^{II}_2L(\mu_{1,1}\text{-}NO_3)(H_2O)(NO_3)](NO_3)$ (**1**) contain μ-phenoxo-$\mu_{1,1}$-azide and μ-phenoxo-$\mu_{1,1}$-nitrate dicopper(II) cores, respectively. However, no peak corresponding to a species having a μ-phenoxo-$\mu_{1,1}$-azide or μ-phenoxo-$\mu_{1,1}$-nitrate bridging moiety is observed in the ESI-MS positive spectra. On the other hand, the spectra of **1** and **4** are similar to that of the μ-phenoxo-μ-hydroxo dicopper(II) compound **2**. Clearly, positive ions having μ-phenoxo-$\mu_{1,1}$-azide dicopper(II) and μ-phenoxo-$\mu_{1,1}$-nitrate dicopper(II) cores in this ligand system are practically very unstable in comparison to the μ-phenoxo-μ-hydroxo dicopper(II) cores in the ESI-MS positive time scale, and therefore, a positive ion having a μ-phenoxo-μ-hydroxo dicopper(II) core is produced for all three compounds resulting in similar spectra.

To get an insight to the nature of possible complex−substrate intermediate, ESI-MS positive spectra of a 1:100 mixture of complex **2** and 3,5-DTBCH$_2$ were recorded after 5 min of mixing. This observed spectra along with simulated patterns are presented in Figure 16. In this case, five peaks are observed at

dx.doi.org/10.1021/ic200409d |*Inorg. Chem.* 2011, 50, 7540–7554

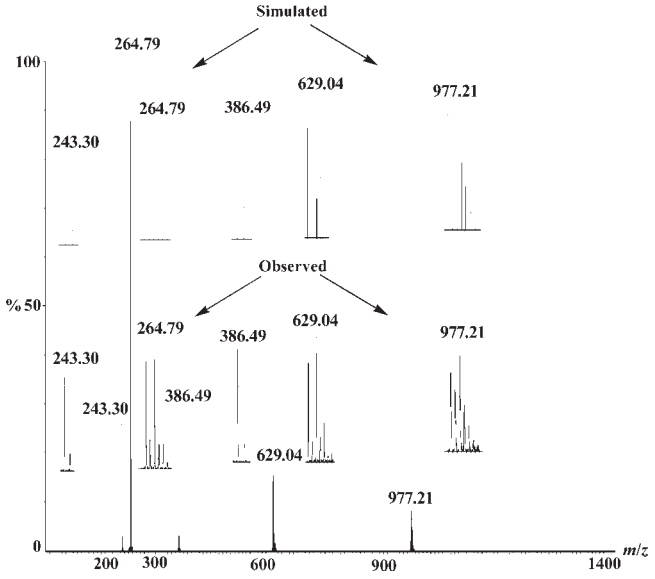

Figure 16. Electrospray mass spectra (ESI-MS positive) of a 1:100 mixture of $[\{Cu^{II}_2L(\mu\text{-}OH)(H_2O)\}(\mu\text{-}ClO_4)]_n(ClO_4)_n$ (**2**) and 3,5-DTBCH$_2$ in acetonitrile recorded after 5 min of mixing, showing observed and simulated isotopic distribution pattern.

m/z = 243 (28%, line to line separation 1.0), 264 (100%, line to line separation 0.5), 387 (31%, line to line separation 1.0), 629 (17%, line to line separation 1.0), and 977 (10%, line to line separation 1.0). Among these, the peaks at 264 and 629 are same as in the spectrum of complex **2**. Of the remaining three peaks, the signal at 243 is well assignable to the quinone−sodium aggregate $[3,5\text{-DTBQ-Na}]^+$ ($C_{14}H_{20}O_2Na$), while the peak at 387 arises because of the monoprotonated ligand $[LH_2]^+$ ($C_{24}H_{27}N_4O$) in which probably both the imine nitrogen atoms are protonated. The remaining peak at 977 is quite interesting because the peak position and matching of the isototropic distribution of the observed and simulated patterns (Figure 16) clearly indicate that this peak arises because of the 1:2 complex−substrate−sodium aggregate $[Cu^{II}_2L(3,5\text{-DTBC}^{2-})(3,5\text{-DTBCH}^-)Na^I]^+$ ($C_{52}H_{66}N_4O_5Cu_2Na$). It has been already discussed that, in addition to the endogeneous bridging phenoxo oxygen atom of L^-, one exogeneous bridging group (nitrate in **1**, hydroxo in **2** and **5**, and azide in **4** and **5**) potentially bridges two copper(II) centers, and therefore, it is more probable that the 3,5-DTBC^{2-} and 3,5-DTBCH$^-$ moieties in $[Cu^{II}_2L(3,5\text{-DTBC}^{2-})(3,5\text{-DTBCH}^-)Na]^+$ behave as an exogeneous bridging ligand and a monodentate ligand, respectively. Thus the positive ion can be better formulated as $[Cu^{II}_2L(\mu\text{-}3,5\text{-DTBC}^{2-})(3,5\text{-DTBCH}^-)Na]^+$

It is relevant to briefly mention at this stage the type of complex−substrate aggregates reported previously. Using tetrachlorocatechol ($TCCH_2$) as the substrate, crystal structures of a few 1:1 dicopper(II)-TCC^{2-} systems are known in which TCC^{2-} acts as a bridging ligand through its two anionic oxygen atoms.[29a] With the same substrate[29b] and also with 3,4-dihydroxy-methylbenzoate,[22] a few 1:2 dicopper(II)-TCC^{2-} systems have also been characterized crystallographically; in these compounds, each TCC^{2-} acts as a chelating ligand for a copper(II) center. Using inactive *p*-nitrocatechol, one example of a 1:2 dicopper(II)-substrate aggregate having dinegative chelating substrate has been characterized by UV−vis spectroscopic studies.[29c] Existence of a 1:2 dicopper(II)−substrate aggregate, with 3,5-$DTBCH_2$ as the substrate, has also been claimed from UV−vis spectroscopic studies.[29d] Clearly, in all the established complex−substrate aggregates, the catechole moiety is linked in its dideprotonated dinegative form and binds the metal centers either as a bridging ligand or as a chelating ligand. Therefore, the existence of $[Cu^{II}_2L(\mu\text{-}3,5\text{-DTBC}^{2-})(3,5\text{-DTBCH}^-)Na^I]^+$ having both the di- and mononegative forms as well as having both the bridging and monodentate modes of the catechol moiety can be considered as an interesting observation.

Two catalytic mechanisms of the catecholase activity have been proposed, one by Kreb's group[13f,13g] and another by Solomon's group.[13d] In both these two mechanisms, 1:1 adduct formation between a dicopper(II) core and the substrate has been mentioned. However, the main difference between the two mechanistic proposals involves the binding mode of the substrate to the dicopper(II) core; whereas a monodentate asymmetric coordination of the substrate was proposed by Krebs and co-workers, a simultaneous coordination of the substrate to both copper centers in the dinucleating bridging fashion is suggested by Solomon et al. As mentioned above, a complex−substrate aggregate $[Cu^{II}_2L(\mu\text{-}3,5\text{-DTBC}^{2-})(3,5\text{-DTBCH}^-)Na^I]^+$ having both a bridging bidentate (as in Solomon's mechanism) and a monodentate (as in Kreb's mechanism) catechol moiety has been identified in ESI-MS positive spectrum. However, as applicable to solid state structures, the ESI-MS positive stabilized aggregates may not be considered as a real intermediate in the course of catecholase activity because these aggregates are stabilized in the time scale of the spectrum and as a positive ion. Nontheless, the aggregate identified here deserves importance because this is clear evidence of the coordination and bridging ability of the substrate to the complexes, which is essentially required for catecholase activity.

CONCLUSIONS

One aim of the present investigation has been to derive complexes having a new type of composition and topology by utilizing new organic blocking ligands in combination with secondary ligands, azide in particular. As anticipated, we have isolated two azide-containing compounds, tetranuclear compound **4** and heptanuclear-based 1-D compound **5**, both having new types of structures in the family containing numerous azide compounds of any metal ion. Again, compound **1** is the sole example to have a μ-phenoxo-$\mu_{1,1}$-nitrate bridging moiety. Thus, new types of structures have been isolated on designing a new ligand. All five complexes exhibit overall antiferromagnetic interaction. Compound **5** may be considered as a nice example to simplify qualitatively the quantitatively complicated situation on applying the magneto−structural correlations. An important aspect of the present investigation is the catecholase activity by three complexes **2**, **4**, and **5**. To the best of our knowledge, the tetranuclear compound **4** and heptacopper(II)-based and dicopper(II)-based one-dimensional compounds, **5** and **2**, are the sole examples of multicopper(II) systems employed to check the possibility of catecholase activity and also to respond positively. Although ESI-MS positive spectra may apparently indicate that a μ-phenoxo-μ-hydroxo dicopper(II) core is responsible for catecholase activity of the tetracopper(II) compound **4** and heptacopper(II) compound **5**, conductance measurements reveal that the active species to initiate catecholase activity for **4** and **5** are most probably Cu^{II}_4 and Cu^{II}_5 moieties, respectively. The observation deserves

dx.doi.org/10.1021/ic200409d |*Inorg. Chem.* 2011, 50, 7540–7554

importance because it opens the utilization of copper(II) clusters and polymers to mimic the biocatalysis. In ESI-MS positive spectra, the identification of the rarely observed μ-phenoxo-μ-oxo moiety and the complex−substrate aggregate $[Cu^{II}_2L(\mu\text{-}3,5\text{-}DTBC^{2-})(3,5\text{-}DTBCH^{-})Na^{I}]^{+}$ should be considered as other two interesting outcomes of the present study.

■ ASSOCIATED CONTENT

Supporting Information. Crystallographic data of **1**−**5** in CIF format, Table S1−S6 and Figures S1−S11. These materials are available free of charge via the Internet at http://pubs.acs.org.

■ AUTHOR INFORMATION

Corresponding Author

*E-mail: sm_cu_chem@yahoo.co.in (S.M.), carolina.sanudo@qi.ub.es. (E.C.S).

■ ACKNOWLEDGMENT

Financial support from the Government of India through the Department of Science and Technology (SR/S1/IC-12/2008), Council for Scientific and Industrial Research (fellowships to S. Majumder), and University Grants Commission (fellowships to S. Sarkar and S. Sasmal) is gratefully acknowledged. Crystallography was performed at the DST-FIST, India-funded Single Crystal Diffractometer Facility at the Department of Chemistry, University of Calcutta. E.C.S. acknowledges the financial support from the Spanish Government, (Grant CTQ2006/03949BQU and Juan de la Cierva fellowship).

■ REFERENCES

(1) (a) Kahn, O. *Molecular Magnetism*; VCH Publications: New York, 1993. (b) *Single-Molecule Magnets and Related Phenomena*; Winpenny, R., Ed.; Springer: New York, 2006. (c) *Magnetism: Molecules to Materials II*; Miller, J. S., Drillon, M., Eds.; Willey-VCH: Weinheim, Germany, 2001.

(2) (a) Papatriantafyllopoulou, C.; Stamatatos, T. C.; Wernsdorfer, W.; Teat, S. J.; Tasiopoulos, A. J.; Escuer, A.; Perlepes, S. P. *Inorg. Chem.* **2010**, *49*, 10486–10496. (b) Alborés, P.; Rentschler, E. *Angew. Chem., Int. Ed.* **2009**, *48*, 9366–9370.

(3) Following references and the references therein: (a) Sasmal, S.; Hazra, S.; Kundu, P.; Majumder, S.; Aliaga-Alcalde, N.; Ruiz, E.; Mohanta, S. *Inorg. Chem.* **2010**, *49*, 9517–9526. (b) Koner, R.; Hazra, S.; Fleck, M.; Jana, A.; Lucas, C. R.; Mohanta, S. *Eur. J. Inorg. Chem.* **2009**, 4982–4988. (c) Sun, H.-L.; Wang, Z.-M.; Gao, S. *Chem. —Eur. J.* **2009**, *15*, 1757–1764. (d) Manca, G.; Cano, J.; Ruiz, E. *Inorg. Chem.* **2009**, *48*, 3139–3144. (e) Serna, Z. E.; Cortés, R.; Urtiaga, M. K.; Barandika, M. G.; Lezama, L.; Arriortua, M. I.; Rojo., T. *Eur. J. Inorg. Chem.* **2001**, 865–872.

(4) (a) Kahn, O.; Mallah, T. *J. Chem. Soc., Dalton Trans.* **1989**, 1117–1126. (b) Cheng, P.; Liao, D.; Yan, S.; Jiang, Z.; Wang, G.; Yao, X.; Wang, H. *Inorg. Chim. Acta* **1996**, *248*, 135–137. (c) Benzekri, A.; Dubourdeaux, P.; Latour, J.-M.; Laugier, J.; Rey, P. *Inorg. Chem.* **1988**, *27*, 3710–3716.

(5) (a) Mallah, T.; Kahn, O.; Gouteron, J.; Jeannin, S.; Jeannin, Y.; O'Connor, C. J. *Inorg. Chem.* **1987**, *26*, 1375–1380. (b) Banerjee, A.; Singh, R.; Colacio, E.; Rajak, K. K. *Eur. J. Inorg. Chem.* **2009**, 277–284. (c) Boillot, M.-L.; Kahn, O.; O'Connor, C. J.; Gouteron, J.; Jeannin, S.; Jeannin, Y. *J. Chem. Soc., Chem. Commun.* **1985**, 178–180.

(6) Tandon, S. S.; Thompson, L. K.; Manuel, M. E.; Bridson, J. N. *Inorg. Chem.* **1994**, *33*, 5555–5570.

(7) Chou, Y.-C.; Huang, S.-F.; Koner, R.; Lee, G.-H.; Wang, Y.; Mohanta, S.; Wei, H.-H. *Inorg. Chem.* **2004**, *43*, 2759–2761.

(8) Thompson, L. K.; Mandal, S. K.; Tandon, S. S.; Bridson, J. N.; Park, M. K. *Inorg. Chem.* **1996**, *35*, 3117–3125.

(9) (a) Sorrell, T. N.; Jameson, D. L.; O'Connor, C. J. *Inorg. Chem.* **1984**, *23*, 190–195. (b) O'Connor, C. J.; Firmin, D.; Pant, A. K.; Babu, B. R.; Stevens, E. D. *Inorg. Chem.* **1986**, *25*, 2300–2307. (c) Lorösch, J.; Hasse, W. *Inorg. Chim. Acta* **1985**, *108*, 35–40. (d) Banerjee, A.; Sarkar, S.; Chopra, D.; Colacio, E.; Rajak, K. K. *Inorg. Chem.* **2008**, *47*, 4023–4031. (e) Lorösch, J.; Quotschalla, U.; Hasse, W. *Inorg. Chim. Acta* **1987**, *131*, 229–236. (f) Mallah, T.; Boillot, M.-L.; Kahn, O.; Gouteron, J.; Jeannin, S.; Jeannin, Y. *Inorg. Chem.* **1986**, *25*, 3058–3065.

(10) (a) Choudhury, C. R.; Dey, S. K.; Karmakar, R.; Wu, C.-D.; Lu, C.-Z.; EJ Fallah, M. S.; Mitra, S. *New. J. Chem.* **2003**, *27*, 1360–1366. (b) Bertoncello, K.; Fallon, G. D.; Hodgkin, J. H.; Murray, K. S. *Inorg. Chem.* **1988**, *27*, 4750–4758.

(11) (a) Transition Metals in Supramolecular Chemistry. In *Perspectives in Supramolecular Chemistry 5*; Sauvage, J.-P., Ed.; Wiley: London, 1999. (b) Zaworotko, M. J. *J. Am. Chem. Soc.* **2010**, *132*, 7821–7822. (c) Zhang, J. J.; Wojtas, L.; Larsen, R. W.; Eddaoudi, M.; Zaworotko, M. J. *J. Am. Chem. Soc.* **2009**, *131*, 17040–17041.

(12) (a) Nayak, M.; Koner, R.; Lin, H.-H.; Flörke, U.; Wei, H.-H.; Mohanta, S. *Inorg. Chem.* **2006**, *45*, 10764–10773. (b) Nayak, M.; Jana, A.; Fleck, M.; Hazra, S.; Mohanta, S. *CrystEngComm* **2010**, *12*, 1416–1421.

(13) (a) Koval, I. A.; Gamez, P.; Belle, C.; Selmeczi, K.; Reedijk, J. *Chem. Soc. Rev.* **2006**, *35*, 814–840. (b) Selmeczi, K.; Reglier, M.; Giorgi, M.; Speier, G. *Coord. Chem. Rev.* **2003**, *245*, 191–201. (c) Than, R.; Feldmann, A. A.; Krebs, B. *Coord. Chem. Rev.* **1999**, *182*, 211–241. (d) Solomon, E. I.; Sundaram, U. M.; Machonkin, T. E. *Chem. Rev.* **1996**, *96*, 2563–2606. (e) Kitajima, N.; Moro-oka, Y. *Chem. Rev.* **1994**, *94*, 737–757. (f) Klabunde, T.; Eicken, C.; Sacchettini, J. C.; Krebs, B. *Nat. Struct. Biol.* **1998**, *5*, 1084–1090. (g) Eicken, C.; Krebs, B.; Sacchettini, J. C. *Curr. Opin. Struct. Biol.* **1999**, *9*, 677–683.

(14) (a) Reim, J.; Krebs, B. *J. Chem. Soc., Dalton Trans.* **1997**, 3793–3804. (b) Rey, N. A.; Neves, A.; Bortoluzzi, A. J.; Pich, C. T.; Terenzi, H. *Inorg. Chem.* **2007**, *46*, 348–350. (c) Belle, C.; Beguin, C.; Gautier-Luneau, I.; Hamman, S.; Philouze, C.; Pierre, J. L.; Thomas, F.; Torelli, S. *Inorg. Chem.* **2002**, *41*, 479–491. (d) Anekwea, J.; Hammerschmidta, A.; Rompelb, A.; Krebs, B. *Z. Anorg. Allg. Chem.* **2006**, *632*, 1057–1066. (e) Ackermann, J.; Meyer, F.; Kaifer, E.; Pritzkow, H. *Chem.—Eur. J.* **2002**, *8*, 247–258. (f) Mukherjee, J.; Mukherjee, R. *Inorg. Chim. Acta* **2002**, *337*, 429–438. (g) Ghosh, D.; Lal, T. K.; Ghosh, S.; Mukherjee, R. *J. Chem. Soc. Chem. Commun.* **1996**, 13–14. (h) Ghosh, D.; Mukherjee, R. *Inorg. Chem.* **1998**, *37*, 6597–6605.

(15) (a) Merkel, M.; Mçller, N.; Piacenza, M.; Grimme, S.; Rompel, A.; Krebs, B. *Chem.—Eur. J.* **2005**, *11*, 1201–1209. (b) Fernandes, C.; Neves, A.; Bortoluzzi, J.; Mangrich, A. S.; Rentschler, E.; Szpoganicz, B.; Schwingel, E. *Inorg. Chim. Acta* **2001**, *320*, 12–21. (c) Neves, A.; Rossi, L. M.; Bortoluzzi, A. J.; Mangrich, A. S.; Haase, W.; Werner, R. *J. Braz. Chem. Soc.* **2001**, *12*, 747–754.

(16) Nanda, P. K.; Bertolasi, V.; Aromí, G.; Ray, D. *Polyhedron* **2009**, *28*, 987–993.

(17) Gupta, R.; Mukherjee, S.; Mukherjee, R. *Polyhedron* **2000**, *19*, 1429–1435.

(18) Majumder, A.; Goswami, S.; Batten, S. R.; El Fallah, M. S.; Ribas, J.; Mitra, S. *Inorg. Chim. Acta* **2006**, *359*, 2375–2382.

(19) Kao, C.-H.; Wei, H.-H.; Liu, Y.-H; Lee, G.-H; Wang, Y.; Lee, C.-J. *J. Inorg. Biochem.* **2001**, *84*, 171–178.

(20) Thirumavalavan, M.; Akilan, P.; Kandaswamy, M.; Chinnakali, G.; Senthil Kumar, G.; Fun, H. K. *Inorg. Chem.* **2003**, *42*, 3308–3317.

(21) Smith, S. J.; Noble, C. J.; Palmer, R. C.; Hanson, G. R.; Schenk, G.; Gahan, L. R.; Riley, M. *J. Biol. Inorg. Chem.* **2008**, *13*, 499–510.

(22) Manzur, J.; García, A. M.; Vega, A.; Ibañez, A. *Polyhedron* **2007**, *26*, 115–122.

(23) (a) Mallah, T.; Boillot, M.-L.; Khan, O.; Gouteron, J.; Jeannin, S.; Jeannin, Y. *Inorg. Chem.* **1986**, *25*, 3058–3065. (b) O'Connor, C. J.; Firmin, D.; Pant, A. K.; Babu, B. R.; Stevens, E. D. *Inorg. Chem.* **1986**, *25*, 2300–2307. (c) Gagne, R. R.; Kreh, R. P.; Dodge, J. A. *J. Am. Chem. Soc.* **1979**, *101*, 6917–7822. (d) Khan, O.; Mallah, T.; Gouteron, J.; Jeannin, S.; Jeannin, Y. *J. Chem. Soc., Dalton Trans.* **1989**, 1117–1126.

(24) (a) Visinescu, D.; Pascu, G. I.; Andruh, M.; Magull, J.; Roesky, H. W. *Inorg. Chim. Acta* **2002**, *340*, 201–206. (b) Visinescu, D.; Madalan, A. M.; Kravtsov, V.; Simonov, Y. A.; Schmidtmann, M.; Müller, A.; Andruh, M. *Polyhedron* **2003**, *22*, 1385–1389.

(25) (a) Tandon, S. S.; Bunge, S. D.; Motry, D.; Costa, J. S.; Aromí, G.; Reedijk, J.; Thompson, L. K. *Inorg. Chem.* **2009**, *48*, 4873–4881. (b) Tandon, S. S.; Bunge, S. D.; Patel, N.; Thompson, L. K. *Inorg. Chem. Commun.* **2009**, *12*, 1077–1080.

(26) Ullman, F.; Brittner, K. *Chem. Ber.* **1909**, *42*, 2539–2548.

(27) (a) *APEX-II, SAINT-Plus, and TWINABS*; Bruker−Nonius AXS, Inc.: Madison, WI, 2004 (b) Sheldrick, G. M. *SAINT*, version 6.02 and *SADABS*, version 2.03; Bruker AXS, Inc.: Madison, WI, 2002. (c) *SHELXTL*, version 6.10; Bruker AXS, Inc.: Madison, WI, 2002. (d) Sheldrick, G. M. *SHELXL-97, Crystal Structure Refinement Program*; University of Göttingen: Germany, 1997.

(28) Geary, W. J. *Chem. Rev.* **1971**, *7*, 81–122.

(29) (a) Karlin, K. D.; Gultneh, Y.; Nicholson, T.; Zubieta, J. *Inorg. Chem.* **1985**, *24*, 3725–3727. (b) Börzel, H.; Comba, P.; Pritzkow, H. *Chem. Commun.* **2001**, 97–98. (c) Plenge, T.; Dillinger, L.; Santagostini, L.; Casella, L.; Tuczek, F. *Z. Anorg. Allg. Chem.* **2003**, *629*, 2258–2265. (d) Torelli, S.; Belle, C.; Hamman, S.; Pierre, J.-L.; Saint-Aman, E. *Inorg. Chem.* **2002**, *41*, 3983–3989.